الجمهورية الجزائرية الديمقراطية الشعبية

DEMOCRATIC AND POPULAR ALGERIAN REPUBLIC

وزارة التعليم العالي والبحث العلمي

MINISTRY OF HIGHER EDUCATION AND SCIENTIFIC RESEARCH

جامعة الشهيد حمه لخضر الوادي

ECHAHID HAMMA LAKHDAR UNIVERSITY OF EL-OUED

كلية التكنولوجيا

Faculty of Technology

قسم الهندسة الكهربائية

Department of Electrical Engineering

Master 's Thesis

In order to obtain an Academic Master's diploma in Technology

Specialty: Telecommunications Systems

Title

Comparative Study Of Advanced Modulation Tachniques Of Wdm Fso System Under Combined Desert Impairments

Presented by:

MEDJOUEL elhadj djilani

Jury Members:

President: Dr.prof.KAHELIL Abd Ellatif	Pr	El-Oued University
Examiner: Dr.TINEDERT Imad Eddine	MCA	El-Oued University
Supervisor: Dr. HADJADJI Narimane	MCA	El-Oued University

University year: 2025/2026

Acknowledgments

First and foremost, I am deeply grateful to the Almighty for granting me the resilience and wisdom to successfully navigate this journey of knowledge and growth.

I extend my heartfelt thanks and appreciation to my supervisor, HADJADJI Narimane, for her exceptional guidance, patience, and boundless support. Her insightful feedback and continuous encouragement were essential to the success of this research.

I would also like to acknowledge all the faculty members and mentors who contributed to my academic development, as well as everyone who supported me, near or far, throughout this transformative experience. I truly cherish this milestone, which I hope will serve as a fruitful contribution to the field of wired and wireless telecommunication systems.

Dedication

…

Abstract

This research presents a comprehensive modeling and performance evaluation of an 8-channel Wavelength Division Multiplexing Free-Space Optical) communication system designed to operate under the severe atmospheric dynamics of El Oued Province, Algeria. Utilizing OptiSystem simulation software, the study compares the resilience and spectral efficiency of advanced coherent modulation formats, specifically Dual-Polarization 16-State Quadrature Amplitude Modulation) operating at 112 Gbps per channel and DP-QPSK operating at 112 Gbps per channel. The atmospheric channel is rigorously modeled to account for thermal turbulence using the Gamma-Gamma distribution, and attenuation via the Beer-Lambert law across five meteorological states: clear skies, light rain, heavy rain, dust storms, and severe dust storms. Performance evaluations across different tiers or configurations of the same 8-channel FSO WDM system labeled as Range A, B, and Creveal a fundamental operational trade-off. While DP-16QAM maximizes data capacity and spectral efficiency, it is highly susceptible to Mie scattering and phase noise under dense particulate conditions. Conversely, DP-QPSK demonstrates superior link robustness and tolerance to signal degradation. The findings underscore that maintaining multi-Gbps optical connectivity in challenging desert environments necessitates strategic modulation selection to overcome drastic reductions in transmission range.

Keywords: DP-16QAM, DP-QPSK, Atmospheric Attenuation, Thermal Turbulenc, Dust Storms.

الملخص

يقدم هذا البحث نمذجة شاملة وتقييماً لأداء نظام اتصالات بصري في الفضاء الحر بتقنية التعدد الإرسالي بتقسيم الطول الموجي بـ 8 قنوات، والمصمم للعمل في ظل الديناميكيات الجوية القاسية لولاية الوادي بالجزائر. باستخدام برنامج المحاكاة OptiSystem، تقارن الدراسة بين مرونة وكفاءة الطيف لتنسيقات التضمين المتماسك المتقدمة، وتحديداً التضمين السعوي المتعامد ذو 16 حالة ثنائي الاستقطاب الذي يعمل بسرعة 112 جيجابت في الثانية لكل قناة، و DP-QPSK الذي يعمل بسرعة 112 جيجابت في الثانية لكل قناة. تمت نمذجة القناة الجوية بدقة لأخذ الاضطرابات الحرارية في الاعتبار باستخدام توزيع جاما-جاما، والتوهين عبر قانون بير-لامبرت عبر خمس حالات جوية: السماء الصافية، المطر الخفيف، المطر الغزير، العواصف الترابية، والعواصف الترابية الشديدة. تكشف تقييمات الأداء عبر مستويات أو تكوينات مختلفة لنفس نظام ذي الـ 8 قنوات، والمصنفة كنطاقات ، عن مفاضلة تشغيلية أساسية. في حين أن يزيد من سعة البيانات والكفاءة الطيفية إلى أقصى حد، فإنه شديد التأثر بتشتت ماي وضوضاء الطور في ظل ظروف الجسيمات الكثيفة. وعلى العكس من ذلك، يُظهر متانة فائقة للرابط وتسامحاً مع تدهور الإشارة. تؤكد النتائج على أن الحفاظ على اتصال بصري بسرعات جيجابت متعددة في البيئات الصحراوية الصعبة يتطلب اختياراً استراتيجياً للتضمين للتغلب على الانخفاضات الجذرية في مسافة الإرسال.

الكلمات المفتاحية : DP-16QAM، DP-QPSK، التوهين الجوي، الاضطرابات الحرارية، العواصف الترابية.

Résumé

Cette recherche présente une modélisation complète et une évaluation des performances d'un système de communication optique en espace libre à multiplexage par répartition en longueur d'onde à 8 canaux, conçu pour fonctionner sous les dynamiques atmosphériques sévères de la wilaya d'El Oued, en Algérie. En utilisant le logiciel de simulation OptiSystem, l'étude compare la résilience et l'efficacité spectrale des formats de modulation cohérente avancés, spécifiquement la modulation d'amplitude en quadrature à 16 états à double polarisation fonctionnant à 112 Gbps par canal et la DP-QPSK fonctionnant à 112 Gbps par canal. Le canal atmosphérique est rigoureusement modélisé pour tenir compte de la turbulence thermique à l'aide de la distribution Gamma-Gamma, et de l'atténuation via la loi de Beer-Lambert à travers cinq états météorologiques : ciel clair, pluie légère, pluie forte, tempêtes de poussière et tempêtes de poussière sévères. Les évaluations des performances sur différents niveaux ou configurations du même système WDM FSO à 8 canaux, étiquetés Plage A, B et C, révèlent un compromis opérationnel fondamental. Bien que la DP-16QAM maximise la capacité de données et l'efficacité spectrale, elle est très sensible à la diffusion de Mie et au bruit de phase dans des conditions de particules denses. À l'inverse, la DP-QPSK démontre une robustesse de liaison et une tolérance supérieures à la dégradation du signal. Les résultats soulignent que le maintien d'une connectivité optique multi-Gbps dans des environnements désertiques difficiles nécessite une sélection stratégique de la modulation pour surmonter les réductions drastiques de la portée de transmission.

Mots-clés : DP-16QAM, DP-QPSK, Atténuation atmosphérique, Turbulence thermique, Tempêtes de poussière.

Table of Contant

Chapter II: Principles of Optical Propagation in Free Space

Chapter III: Advanced Modulation Techniques for Desert WDM-FSO

Figures List

Tables list

List of Mathematical Symbols

λ Wavelength (nm)

μ_1, μ_0 Mean signal levels for bit "1" and "0"

σ_1, σ_0 Noise standard deviations for bit "1" and "0"

Q Quality Factor

BER Bit Error Rate

SNR Signal-to-Noise Ratio

OSNR Optical Signal-to-Noise Ratio

θ Beam divergence angle (mrad)

W_0 Beam waist radius (m)

Z_R Rayleigh range (m)

D Aperture diameter (cm)

R Rain rate (mm/h) or link range (km)

V Atmospheric visibility (km)

α Attenuation coefficient (dB/km)

σ_a Absorption coefficient

σ_s Scattering coefficient

C_n^2 Refractive index structure parameter (m^{-23})

$\beta(\lambda)$ Wavelength-dependent attenuation coefficient

P_signal Signal power

P_noise Noise power

erfc Complementary error function

I In-phase component

Q Quadrature component

M Number of symbols in M-ary modulation

List of Abbreviations

OOK	On-Off Keying
PPM	Pulse Position Modulation
PSK	Phase Shift Keying
BPSK	Binary Phase Shift Keying
QPSK	Quadrature Phase Shift Keying
DP-QPSK	Dual Polarization QPSK
DPSK	Differential Phase Shift Keying
QAM	Quadrature Amplitude Modulation
M-QAM	M-ary Quadrature Amplitude Modulation
DP-16QAM	Dual Polarization 16-State QAM
QAM	QAM
WDM	Wavelength Division Multiplexing
DWDM	Dense Wavelength Division Multiplexing
CWDM	Coarse Wavelength Division Multiplexing
FSO	Free Space Optics
RF	Radio Frequency
LoS	Line of Sight
NLOS	Non-Line of Sight
NRZ	Non-Return-to-Zero
RZ	Return-to-Zero
EDFA	Erbium-Doped Fiber Amplifier
MZM	Mach-Zehnder Modulator
PBS	Polarization Beam Splitter
PBC	Polarization Beam Combiner
AWG	Arrayed Waveguide Grating
DSP	Digital Signal Processing

LO	Local Oscillator
ADC	Analog-to-Digital Converter
DAC	Digital-to-Analog Converter
APD	Avalanche Photodiode
PIN	p-i-n photodiode
MUX	Multiplexer
DEMUX	Demultiplexer
PMD	Polarization Mode Dispersion
RRC	Root-Raised Cosine
ABC	Automatic Bias Control
ISI	Inter-Symbol Interference
FEC	Forward Error Correction
HD-FEC	Hard-Decision FEC
SD-FEC	Soft-Decision FEC
ITU-T	Intl. Telecommunication Union - Telecom Sector
CW	Continuous Wave
QCL	Quantum Cascade Laser
VLC	Visible Light Communication
Li-Fi	Light Fidelity
UV	Ultraviolet
NIR	Near-Infrared
LWIR	Long-Wave Infrared
MIR	Mid-Infrared
GSM	Global System for Mobile Communications
CDMA	Code Division Multiple Access
UMTS	Universal Mobile Telecommunications System

LTE	Long Term Evolution
IoT	Internet of Things
IMT-2000	Intl. Mobile Telecommunications-2000
Tbps	Terabits per second
Gbps	Gigabits per second
AlGaAs	Aluminum Gallium Arsenide

General Introduction

General Introduction

Driven by the surging global demand for high-speed data transmission that has pushed traditional Radio Frequency (RF) networks to their physical and regulatory limits, this thesis investigates Free-Space Optical (FSO) communication integrated with Wavelength Division Multiplexing (WDM) as a high-capacity, secure, and license-free alternative for desert backhaul environments. To systematically address these multi-faceted challenges and evaluate the viability of this optical wireless solution, the structural narrative of this thesis is logically organized into three comprehensive chapters that transition from fundamental paradigm evolutions to rigorous atmospheric modeling and advanced numerical simulations. The investigative journey begins in Chapter 1, which establishes the primary baseline and overarching motivations for this study by meticulously tracing the historical evolution of wireless standardizations from legacy generations to the impending 6G infrastructure, specifically highlighting how rising radio-frequency bottlenecks, high licensing costs, and spectral scarcity demand an immediate shift toward the completely unregulated optical wireless spectrum. This opening chapter further breaks down the physical architecture of an FSO system dissecting transmitter ,optical channels, and coherent receiver while defining the fundamental figures of merit such as Bit Error Rate (BER), Quality Factor (Q-factor), and eye diagram visualizers used to gauge baseline signal integrity before exposure to atmospheric stressors. Building upon this structural foundation, Chapter 2 introduces the complex physical and mathematical realities of the unguided transmission medium by analyzing the precise mechanisms of light propagation through an open atmospheric channel, with a dedicated focus on the extreme environmental realities of the Sahara Desert. This chapter establishes the rigorous mathematical framework necessary to model severe atmospheric impairments, characterizing the destructive impacts of Mie aerosol scattering induced by regional dust storms and Sirocco winds, thermal scintillation driven by intense diurnal solar heating, and geometric pointing errors caused by structural thermal expansions, thereby mapping out the precise mathematical threats to optical phase and amplitude stability. Ultimately, the theoretical models developed in the preceding chapters are practically applied in Chapter 3, which executes the core performance evaluation and comparative analysis of an 8-channel high-speed WDM-FSO system utilizing the professional simulation platform OptiSystem. This final chapter benchmarks the performance limits of advanced Dual-Polarization 16-State Quadrature Amplitude Modulation (DP-16QAM) operating at 112 Gbps per channel against Dual-Polarization Quadrature Phase Shift Keying (DP-QPSK) operating at 112 Gbps per channel across five distinct meteorological states tailored to the climate of El Oued Province, Algeria. By exposing both formats to varying transmission distances and atmospheric attenuation values, Chapter 3 provides key insights into the critical operational trade-off between spectral efficiency and environmental robustness, defining the strategic necessity for Adaptive Coding and Modulation (ACM) systems to guarantee link availability under unpredictable desert conditions.

Chapter I

The Optical Evolution of Wireless

I.1 introduction

Human communication has evolved from primitive signaling methods to sophisticated, interconnected digital networks, a journey defined by the quest for faster, more reliable information exchange. The transition from wired telegraphs and telephones to the discovery of electromagnetic waves revolutionized human connectivity, enabling the birth of modern wireless systems. Throughout the subsequent cellular generations from 1G to 5G and toward 6G the telecommunications industry has continuously pushed the boundaries of spectral efficiency and network capacity.

However, the industry now faces a critical saturation point. Traditional Radio Frequency (RF) systems, while historical workhorses of the mobile era, are increasingly constrained by spectral scarcity, high licensing costs, and significant interference vulnerabilities. As the demand for terabit-level data throughput grows, these RF bottlenecks have necessitated a paradigm shift toward optical wireless communication. This chapter explores that transition, framing Free Space Optics (FSO) not merely as an alternative, but as the foundational technology required to secure high-capacity, license-free links that bypass the congested RF spectrum. By examining the evolution of these technologies, we establish the critical need for the WDM-FSO systems modeled in this research.

I.2 Evolution of Wireless Communication

I.2.1 The Wireless Revolution

Communication is a fundamental human need that has existed since the earliest civilizations, evolving from primitive methods such as smoke signals, drum beats, and carrier pigeons, to written messages carried by relay messengers across vast empires. As technology advanced, the invention of the electric telegraph in 1837 and the telephone in 1876 allowed information to travel through wired networks at extraordinary speeds, fundamentally transforming how people exchanged information across distances. The next great leap came with the discovery of electromagnetic waves, which laid the foundation for wireless communication the ability to transmit information through the air without any physical connection. Pioneers like Heinrich Hertz and Guglielmo Marconi turned this theory into reality in the late 19th century, giving rise to radio broadcasting, military communications, and early mobile radio systems. However, these early wireless systems were limited, expensive, and could serve only a small number of users at a time. The solution came with the revolutionary cellular concept, which divided coverage areas into small cells and enabled frequency reuse, making mass mobile communication feasible for the first time. This breakthrough set the stage for the development of cellular generations standardized, evolving networks from 1G to 6G and beyond each bringing dramatic improvements in speed, capacity, and capability.

The era of 1G, spanning the late 1970s to the early 1990s, marked the dawn of the mobile revolution with analog voice calls from bulky "brick" phones like the Motorola, plagued by poor security and incompatible standards, yet proving the massive demand for wireless communication.

Emerging in the early 1990s, 2G revolutionized the landscape by shifting to digital cellular technology with GSM and CDMA, introducing encrypted voice, SMS text messaging, and basic data services through iconic devices like the Nokia 3310, establishing the foundational architecture for modern networks. Arriving in the early 2000s, 3G ushered in true mobile broadband with packet-switching and always-on connectivity. It was enabling video calling, mobile TV, and the first smartphone internet experiences under IMT-2000 standards like UMTS, creating the essential infrastructure and consumer demand that birthed the mobile app economy.

Launched commercially in the late 2000s, 4G delivered an all-IP, LTE delivered the first true mobile broadband experience fast enough to rival fixed lines, making HD streaming, gaming, and seamless video conferencing routine while reshaping entire industries and becoming the critical digital infrastructure of the 2010s.

Debuting globally around 2019, 5G is far more than a speed upgrade. Operating across low, mid, and high-band millimetre wave spectrum. It delivers enhanced mobile broadband, ultrareliable low-latency communications, and massive IoT connectivity. Through innovations like network slicing, 5G serves as a unified, intelligent fabric the essential nervous system for autonomous systems, smart cities, and the Fourth Industrial Revolution.

Looking toward 2030 and beyond, the vision for 6G and subsequent generations aims to transcend terrestrial limits. By integrating terahertz frequencies, native AI integration, and satellite-terrestrial fusion. Instead, it will enable holographic telepresence, digital twins, brain-computer interfaces,–and quantum-secured networks evolving from a mere utility into a cognitive cyber-physical continuum. This shift will blend the physical and digital worlds to address humanity's grandest challenges.

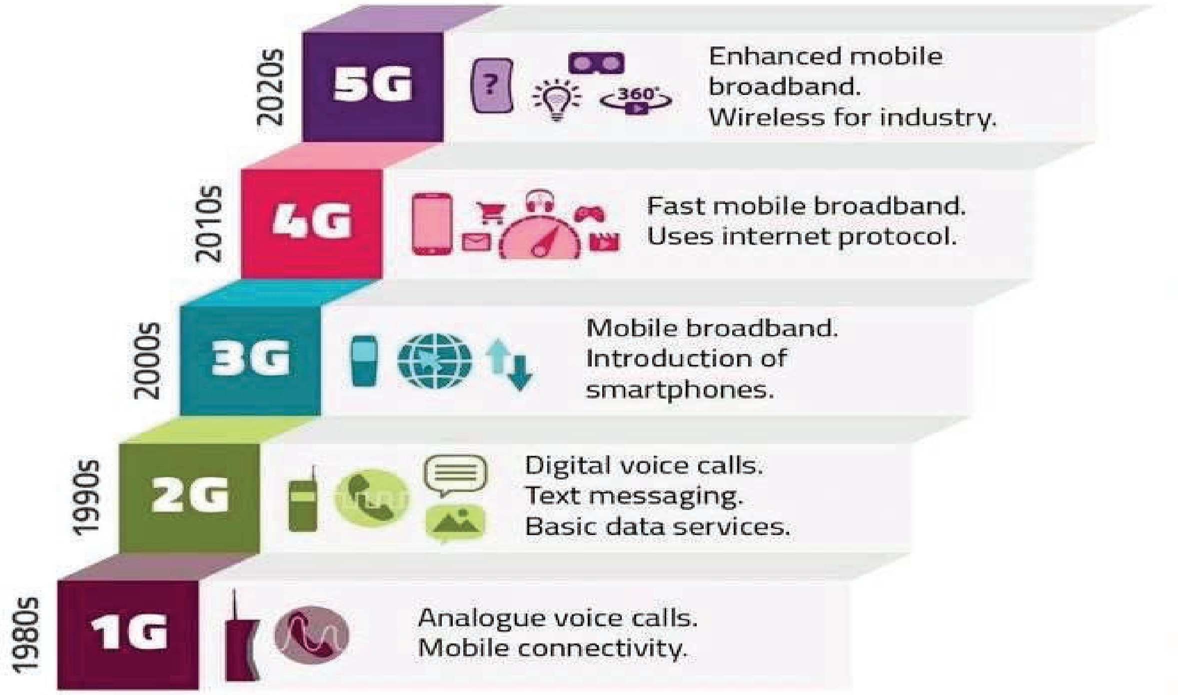

Figure I.1: Evolution of Wireless Communication.

I.3 RF Limitations

Radio Frequency (RF) communication systems are subject to inherent physical and regulatory limitations that constrain their suitability as a long-term solution for high-capacity wireless backhaul. The available RF spectrum is a finite and heavily regulated resource whose allocation imposes significant licensing cost and capacity ceilings that cannot be overcome regardless of advances in hardware or modulation technology. [2]

Moving into the millimeter-wave frequencies where sufficient bandwidth for high-capacity links exists. Hence, the atmospheric absorption and rain fade introduce propagation losses that grow sharply with both link distance and operating frequency. Beyond spectral scarcity, the inherently broad radiation pattern of RF transmissions introduces fundamental security vulnerabilities through susceptibility to interception and jamming. While the transceiver complexity and power consumption required to sustain high data rates translate into considerable infrastructure and operational cost.

This accumulated limitations spectral congestion, distance-dependent, atmospheric degradation, and security exposure that have motivated growing research interest in FSO technology as a complementary or alternative high-capacity wireless solution.

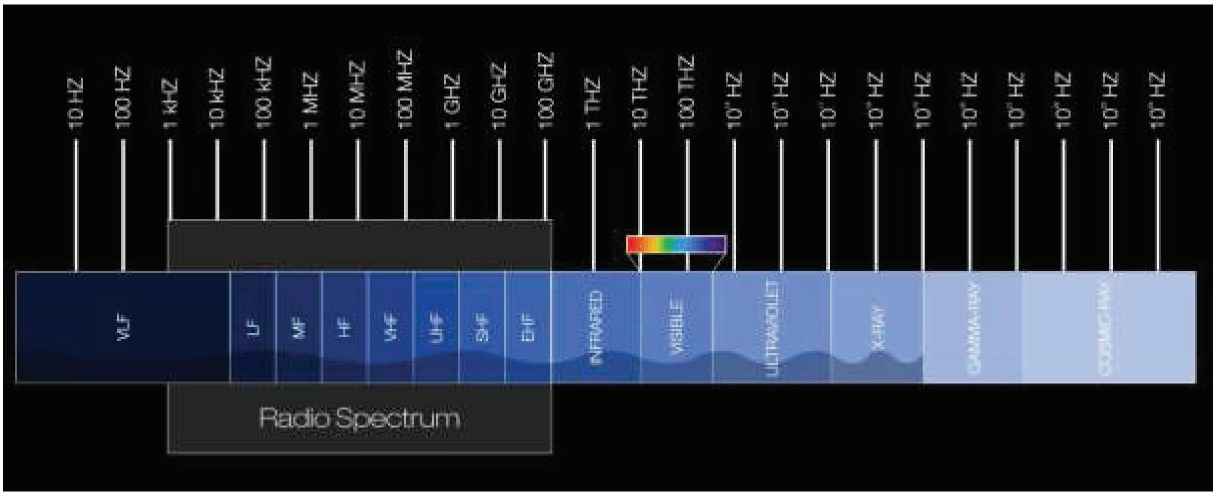

Figure I.2: The RF spectrum.

I.4 The Shift to Optical

The limitations inherent to RF systems have driven a growing shift toward optical wireless communication as a viable alternative for high-capacity link deployment. Free Space Optical technology exploits the vastly wider bandwidth available in the optical spectrum. It is operating at wavelengths in the near-infrared region that are entirely unregulated in most jurisdictions. By eliminating the licensing burden and spectral congestion that constrain RF systems, the directional nature of the optical beam provides an inherent physical layer security advantage that RF cannot replicate without additional complexity. [3], [8]

The maturity of optical fiber component technology, including high-power laser sources, low-noise photodetectors, and wavelength multiplexing devices developed for the telecommunications industry. It has made increasingly practical to translate these components into FSO deployments. In addition, further integration of Wavelength Division Multiplexing into FSO architectures has extended the optical wireless capacity to approach levels of physical fiber infrastructure. This making WDM-FSO a compelling solution for scenarios where fiber deployment is economically or logistically impractical. This convergence of regulatory freedom, directional security, and fiber-compatible capacity represents the fundamental motivation behind the ongoing transition from RF toward optical wireless communication in high-capacity backhaul applications.

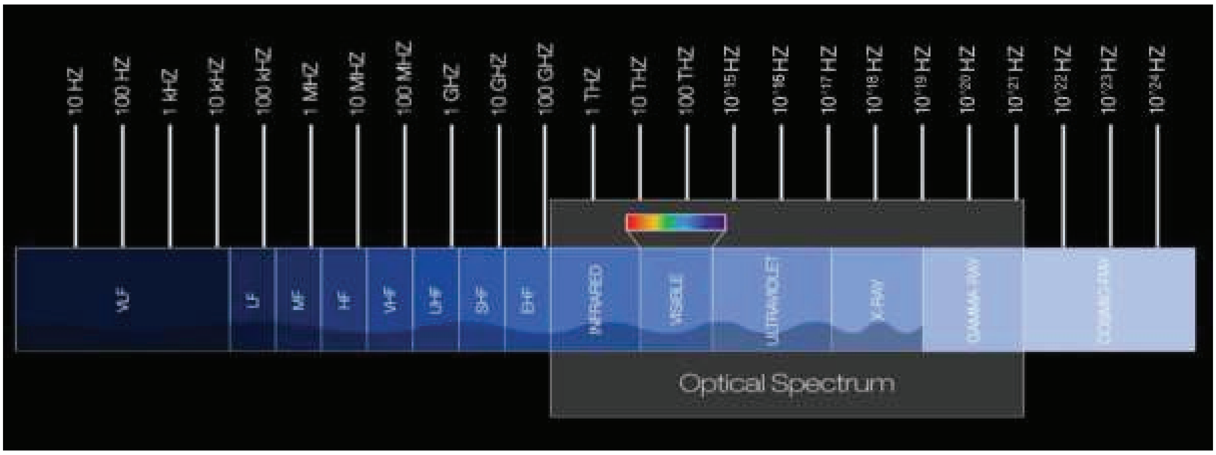

***Figure I.3**: The optical spectrum.*

I.5 Background and Motivation

Global demand for internet services, data transmission, and storage has experienced accelerated growth in recent years. This growth has necessitated the development of advanced communication technologies to meet increasing bandwidth requirements. One of the most prominent technologies is the free space optical communication system integrated with Wavelength Division Multiplexing (WDM-FSO). [1], [6]

Free space optical communication is defined as a wireless communication technology that uses optical beams to transmit data through the atmosphere between transmitting and receiving stations. When integrated with wavelength division multiplexing, it enables the transmission of multiple channels at different wavelengths over the same optical link, significantly multiplying the system's overall capacity. [3]

FSO systems offer a powerful solution for high-bandwidth and security-sensitive needs. Their narrow beam divergence provides enhanced physical security, making any interception attempt easy to detect. Since these systems operate in the optical spectrum, they are entirely immune to RF jamming and electromagnetic interference.

Deployment is also exceptionally fast, requiring only hours instead of the months often needed for fiber optic trenching. Furthermore, license-free operation removes the headache of regulatory hurdles and spectrum fees. Together, these benefits significantly lower both the initial setup costs and the long-term operational expenses.

These advantages make FSO suitable for civilian applications (last-mile connectivity, building-to-building links), military applications (secure tactical communications), and space applications (satellite-to-ground station communications).

Despite their benefits, WDM-FSO systems face major hurdles with atmospheric propagation. Optical signals often experience heavy attenuation and scattering. This is primarily caused by molecular absorption from air and water vapor. Atmospheric turbulence also leads to signal scintillation, which fluctuates the signal strength. [4], [5] [12]

Furthermore, weather phenomenon like fog, rain, and snow significantly disrupt performance. In arid regions, specific desert conditions create additional risks. These include intense dust storms and severe thermal turbulence that can degrade the connection. [10]

To overcome these challenges, advanced modulation techniques (such as DPSK, OFDM, …) are employed to enhance the system's resistance to noise and reduce signal degradation.

Therefore, this research aims to study and evaluate the performance of the WDM-FSO system utilizing different advanced modulation techniques under various impairments in the desert environment of El Oued province. [7]

The deployment of Wavelength Division Multiplexing Free Space Optical (WDM-FSO) communication systems in the desert environment of El Oued, Algeria, is fundamentally constrained by three dominant and simultaneously acting physical impairments that collectively produce channel degradation far exceeding the margins of conventional FSO system design. [10]

The most persistent of these is atmospheric thermal turbulence, sustained by intense Saharan solar heating throughout the daylight hours, which drives the propagation channel into the strong-to-saturated turbulence regime and causes severe randomized irradiance fading across all WDM channels in a manner that existing models developed for temperate climates cannot accurately characterize. Equally damaging, though episodic in nature, is the aerosol extinction caused by frequent dust-laden wind events including the regional Sirocco, which suspends mineral particles whose size overlaps with the operating wavelength band, producing Mie-dominated attenuation that during severe sandstorm events becomes spectrally uniform across the entire WDM channel comb, rendering wavelength-domain diversity strategies ineffective and leaving the link entirely inoperable. [4]

Distinct in its physical origin yet coupled to both preceding mechanisms is the geometric misalignment induced by the extreme diurnal thermal cycling characteristic of the El Oued climate, where in large temperature differentials between night and peak afternoon drive differential structural expansion in the terminal mounting assemblies, generating a cumulative pointing error that compounds the stochastic beam wandering produced by turbulence and progressively erodes coupling efficiency throughout the operational day. Despite the growing relevance of FSO technology for connectivity in underserved arid regions, no unified framework currently exists that jointly characterizes and mitigates all three of these impairments under the specific climatic conditions of the Algerian Sahara, and this gap constitutes the central problem addressed by the present research.

I.6 Research Methodology

This study employs an analytical and simulation-based methodology to evaluate FSO system performance under El Oued Province's climatic conditions using OptiSystem software. The approach integrates local meteorological data from 2025 (temperature, horizontal visibility, and wind speed) with mathematical models to assess atmospheric propagation effects in the desert environment.

I.6.1 Mathematical Modeling and System Design

The simulation model uses OptiSystem software. It follows these specific parameters:

Channel Modeling: The model incorporates Algerian Sahara conditions. It includes dust, sand, turbulence, and Sirocco winds. These factors simulate realistic scattering, absorption, and signal fading.

Application of Physical Laws: The Beer–Lambert Law estimates attenuation levels. The Gamma–Gamma model simulates atmospheric turbulence and thermal scintillation.

I.6.2 Comparative analysis and Performance Evaluation

The methodology ends with a comparative study. It evaluates the system under different climatic scenarios:

The Ideal Scenario: A clear summer day measures heat effects only.

The Critical Scenario: A moderate sandstorm measures light scattering caused by dust.

The results are assessed using key performance indicators. This ensures the proposed system remains reliable.

I.7 Free Space Optical (FSO) Communication

A Free Space Optical (FSO) Communication is a modern wireless communication technology that transmits data by propagating modulated light beams through the open atmosphere, harnessing optical frequencies in the near-infrared spectrum ranging from 780 nm to 1600 nm. Among these, the 1550 nm wavelength stands as the most widely adopted, owing to its inherent eye-safety characteristics and seamless compatibility with established optical fiber components. At its core, an FSO system is built upon three fundamental parts; the transmitter, the free space optical channel, and the receiver. Each one playing an indispensable role in ensuring reliable and high-capacity optical communication.

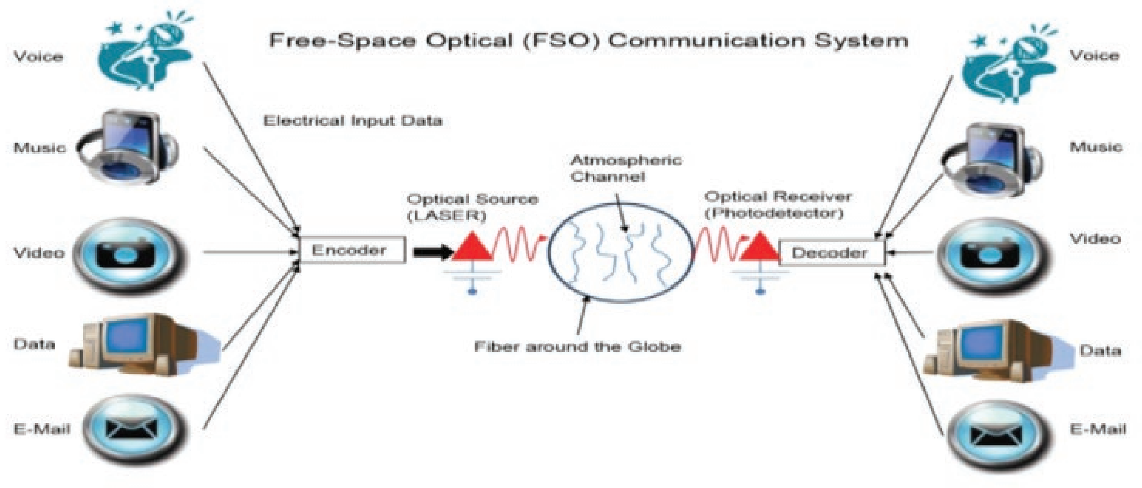

Figure I.4: ***Free Space Optical (FSO) Communication system***.

I.7.1 Transmitter

The transmitter of FSO system consist primarily of laser diodes or LEDs, where laser diodes are overwhelmingly preferred for their high coherence, narrow spectral linewidth, and superior output power. Upon these sources, an electrical data signal is impressed through either direct modulation of the laser drive current, or external modulation via Mach-Zehnder modulators (MZMs). The latter offering superior bandwidth and reduced frequency chirp for high-speed applications.

The resulting optical beam is then collimated and steered toward the target through high-precision telescopic optics, with active beam-steering and fine-pointing assemblies incorporated to compensate for mechanical vibrations and thermal misalignment.

I.7.2 The Free Space Channel

The free space channel represents the heart of the FSO system, where the atmosphere itself becomes the transmission medium through which the optical beam silently travels along a strict line-of-sight path. However, this medium is a complex and ever-changing environment in which atmospheric phenomena such as fog, rain, turbulence, and airborne particles introduce signal attenuation, scattering, and beam wander, rendering the channel the most dynamic and challenging element of the entire system. It is precisely this atmospheric dependency that distinguishes FSO from its wired counterparts and defines the boundaries of its performance.

I.7.3 Receiver

At the far end of the link, the receiver is responsible for collecting and recovering the transmitted optical signal. A telescope or optical aperture gathers the incoming light and directs it onto a photodetector either a PIN photodiode or an avalanche photodiode (APD). Then, it is converted back into its electrical form for processing and decoding. The sensitivity and dynamic range of the receiver are therefore decisive factors in sustaining reliable communication across extended distances and under varying atmospheric conditions.

Figure I.5: (a) FSO transceivers.[16]

FSO transceivers generally operate in two fundamental modes

1. Simplex Mode

Communication flows in only one direction from transmitter to receiver using a single optical beam. This mode is simpler and less costly but limits the link to unidirectional data transfer, making it suitable only for specific applications such as broadcasting or one-way monitoring.

2. Full-Duplex Mode

Two optical beams operate simultaneously in opposite directions, allowing bidirectional communication between two terminals. Each terminal houses both a transmitter and a receiver, enabling simultaneous transmission and reception. This is the most commonly deployed mode in practical FSO systems, as it supports two-way data exchange essential for real-world communication networks.

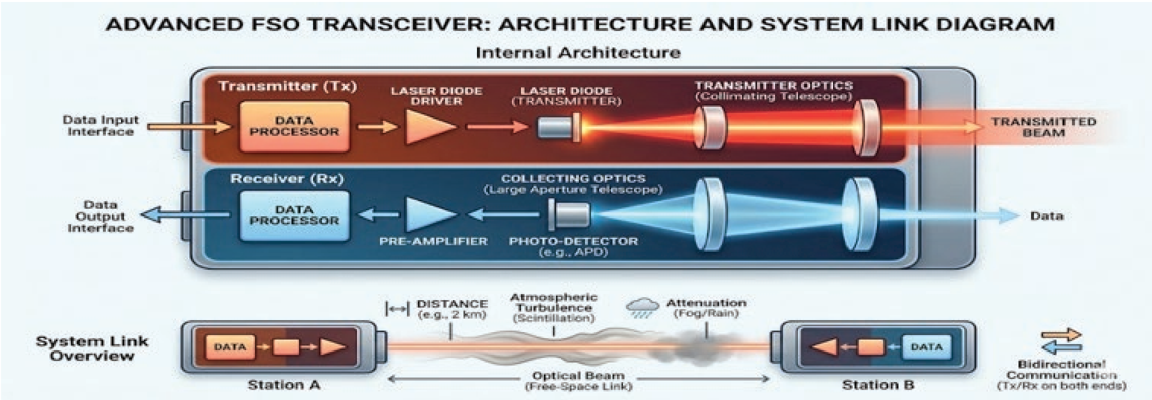

Figure I.6: Advanced FSO transceivers modes.[16]

I.8 Key Advantages of Free Space Optical

While the raw speed of Free-Space Optical (FSO) communication is certainly its headline feature, its practical value in the field often stems from three core advantages over traditional connectivity: cost-efficiency, inherent security, and a lack of spectrum regulation.

- **Cost-Effectiveness**

One of the most compelling reasons to adopt FSO is its economic efficiency, particularly when compared to the alternative of laying optical fiber cable. Deploying fiber often requires digging up roads, obtaining right-of-way permits, and navigating complex urban infrastructure a process that is both time consuming and exorbitantly expensive.

- **High Security**

RF signal jamming are constant threats. Therefore, FSO offers a level of physical layer security that is difficult to match. Traditional radio frequency (RF) networks broadcast signals in a wide pattern, making them vulnerable to interception by unauthorized users with spectrum analyzers.

- **Unlicensed Spectrum**

The radio frequency (RF) spectrum is a crowded and highly regulated resource. Telecom companies must spend billions of dollars in auctions to secure exclusive rights to specific frequencies. Even then, they must coordinate to avoid interference with neighbours.

FSO operates in the optical spectrum, which is completely unlicensed. Deploying an FSO link does not require paying recurring licensing fees, or worrying about interfering with other wireless devices.

While a standalone FSO system offers impressive bandwidth and flexibility, the ever-growing demand for higher data rates has driven the integration of WDM-FSO) technology. This convergence is a natural evolution that multiplies the system's overall capacity by simultaneously transmitting multiple independent data streams through the same free space channel. It is forming a WDM-FSO system capable of delivering fiber-like capacities over wireless links.

I.9 WDM-FSO Systems

A WDM-FSO system is the integration of wavelength division multiplexing technology with Free Space Optical communication. It is enable to transmit simultaneously a multiple independent data streams over distinct optical wavelengths through the same free space channel. By assigning each data channel a unique wavelength within the atmospheric transmission window, the system achieves a dramatic multiplication of transmission capacity without increasing aperture size or requiring additional transceivers. [6], [11]

At the transmitter side, multiple laser sources are operating at a distinct wavelength conforming to the ITU-T grid spacing of 1.6 nm (200 GHz), 0.8 nm (100 GHz), or 0.4 nm (50 GHz). They are independently modulated with separate data streams and then combined into a single composite optical beam using a wavelength multiplexer or optical coupler. This multiplexed beam is subsequently combined and launched into the free space channel as a single transmission. It is carrying all wavelength channels simultaneously through the atmosphere toward the distant receiver.

At the receiver side, the collected composite beam is directed onto a wavelength demultiplexer, which separates the individual wavelength channels. Then, it routes each to its corresponding photodetector for independent detection and decoding. The demultiplexing process must be performed with high spectral precision to prevent inter-channel crosstalk, which can degrade signal quality and introduce bit errors.

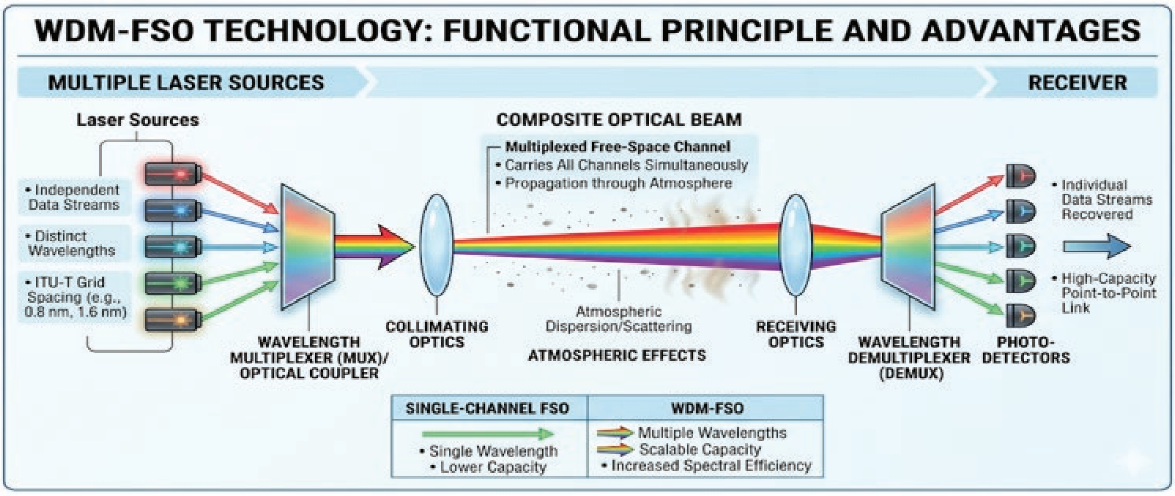

Figure I.7: WDM-FSO System.[16]

WDM-FSO systems are broadly classified into two categories depend on spacing channel:

DWDM Spacing: Dense Wavelength Division Multiplexing (DWDM) typically uses channel spacings of 100 GHz (approx. 0.8 nm) or 50 GHz (approx. 0.4 nm) in the C-band and L-band. It is a high spectral efficiency.

CWDM Spacing: Correct. Coarse WDM (CWDM) uses a 20 nm channel spacing as defined by the ITU-T G.694.2 standard. It simpler and more cost-effective implementation.

Free Space Optics (FSO) combined with DWDM is indeed a solution for high-capacity backhaul (often for 5G/6G and data centers) and metropolitan networks, frequently achieving multi-Tbps aggregates in research and high-end deployments.

I.10 Free Space Optical Applications

FSO technology enabler for many applications. Specifically :

Given the broad range of applications, that FSO technology serves from urban telecommunications and military communications to space links and 5G backhaul. It becomes essential to assess how well these systems perform under real-world conditions. This requires the definition of standardized performance parameters, which provide a quantitative framework for evaluating the reliability, efficiency, and quality of FSO links across different environments and deployment scenarios.

I.11 Performance Metrics for FSO System

To determine how well a free space optical system performs, engineers turn to several main characteristics that capture link reliability, signal quality, and transmission efficiency. These indicators are indispensable they shape the design process, drive optimization efforts. In addition, they provide a basis for meaningful comparison with other communication technologies.

I.11.1. Bit Error Rate (BER)

Bit Error Rate is a foundational performance parameter that quantifies the probability of incorrect bit detection at the receiver, directly reflecting signal integrity. [9]

In free space optical systems, a BER threshold of 10^{-9} is conventionally targeted for reliable, high-quality links. Performance degradation below this threshold can result from atmospheric turbulence, spatial misalignment, or ambient noise interference. Mathematically, BER is defined as the ratio of received bits to the total number of transmitted bits.

I.11.2. Q-Factor

The Q-Factor is a statistical measure of signal quality at the receiver's decision circuit, defined as : [9]

$$Q = \frac{\mu_1 - \mu_0}{\sigma_1 + \sigma_0} \tag{1.1}$$

Where μ represents mean signal levels and σ represents noise standard deviations. It is measured by sampling the received signal, constructing amplitude histograms for "1" and "0" bits, and applying this formula.

The Q-Factor directly relates to bit error rate through:

$$BER = \frac{1}{2}\text{erfc}\left(\frac{Q}{\sqrt{2}}\right) \tag{1.2}$$

A successful FSO link typically requires $Q > 6$, which ensures $BER < 10^{-9}$.

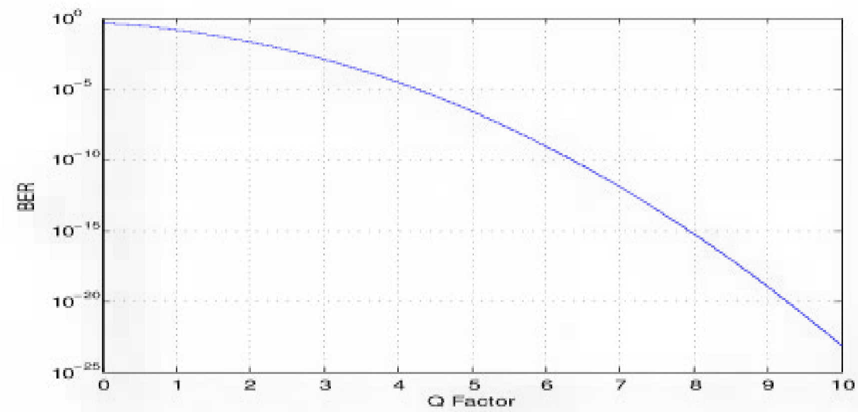

Figure I.8: *BER versus Q factor.*

I.11.3. Signal-to-Noise Ratio (SNR)

The SNR value quantifies signal purity by comparing signal power to noise power, expressed as:

$$SNR = \frac{P_{signal}}{P_{noise}} \quad (1.3)$$

$$SNR\ dB = 10\ log\ 10\ (\frac{P_{signal}}{P_{noise}}) \quad (1.4)$$

Engineers measure it using a spectrum analyzer to compare received signal power against background noise, or estimate it from eye diagrams using amplitude statistics. SNR directly affects bit error rate, which higher SNR means fewer errors.

Successful FSO operation typically requires SNR above 15 dB to maintain reliable detection.

I.11.4. Eye Diagrams

An eye diagram is a visual representation of signal quality created by overlaying thousands of received bit segments on an oscilloscope, synchronized to the data clock. Engineers extract critical metrics from it: [1]

Eye Height (*vertical opening indicating noise margin*), Eye Width (*horizontal opening indicating timing jitter*), and Eye-Opening Penalty (*degradation measurement*).

A wide-open eye with clean transitions confirms low noise, minimal jitter, and sufficient signal integrity.

Conversely, a closed or distorted eye reveals performance degradation from turbulence, misalignment, or interference. In successful FSO systems, the eye diagram provides instant qualitative confirmation of the quantitative measurements from Q-Factor and SNR.

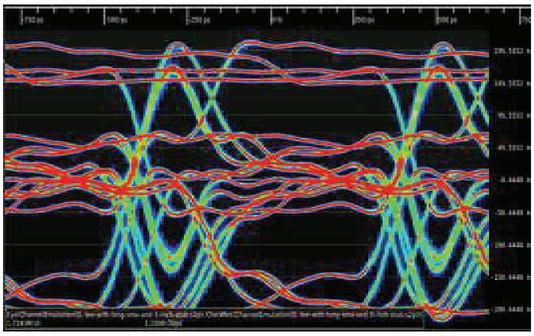

(b)

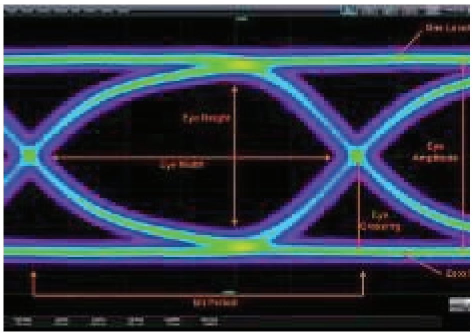

(a)

Figure I.9.: (a) open eye diagram, (b) distorted eye diagram.

I.12. Conclusion

In this chapter it was reviewed the transition from RF to FSO/WDM-FSO technology for 6G and beyond as a high-capacity and license-free solution. As far as the desert region is concerned, the main link impediments are attributable to atmospheric turbulence, extinction due to dust, and geometric misalignment. The first impediment is modeled by Gamma-Gamma theory whereas the second impediment is modeled by Beer-Lambert theory. Through the introduction of critical benchmarks like Bit Error Rate (BER) and Q-Factor, the objective of this study was to furnish a theoretical framework for the performance assessment of high-speed modulation techniques in the harsh Saharan environment.

Chapter II

Principles of Optical Propagation in Free Space

II.1 Introduction

FSO systems use laser propagation through the dynamic and uncontrolled atmosphere. The signals go through certain physical phenomena in the atmosphere affecting the spatial distribution and power on the receiver plane. Optical wave propagation according to electromagnetic wave theory is laid down in this chapter. The frequency ranges that are suitable and the mathematical systems which can help predict the behaviour of the beam and design the system.

II.2 Principles of Optical Propagation in Free Space

II.2.1 Electromagnetic Spectrum and Optical Frequencies in FSO

The electromagnetic spectrum encompasses a vast range of frequencies, from low-frequency radio waves to high-energy gamma rays. Free-Space Optical communication systems operate within the optical portion of this spectrum, utilizing frequencies that offer favorable propagation characteristics through the atmosphere while remaining compatible with available photonic technologies [9], [16].

II.2.1.1 Selection of Optical Frequencies

The choice of operating wavelength in FSO systems is governed by several competing factors. The atmosphere exhibits wavelength-dependent absorption and scattering characteristics, with certain spectral regions offering significantly better transmission than others [3], [13]. These atmospheric transmission windows define the practical operating ranges for FSO links, wherein optical signals can propagate with minimal attenuation under clear-weather conditions.

Beyond atmospheric considerations, the selection of optical frequencies must account for technological maturity and component availability. The development of the telecommunications and data communication industries has driven substantial advances in optical sources, detectors, and related components at specific wavelengths [9]. FSO systems benefit from leveraging these mature technologies, which offer reliability, cost-effectiveness, and well-established performance characteristics.

Safety considerations also play a critical role in frequency selection. Different wavelengths pose varying levels of risk to human vision, with certain frequencies being absorbed by the eye's anterior structures before reaching the retina, while others can penetrate deeply and cause potential retinal damage [6], [17]. Regulatory frameworks governing maximum permissible exposure levels influence the selection of operating wavelengths and the allowable transmitted power levels.

II.2.1.2 Optical Frequency Bands

FSO systems typically employ frequencies within three primary spectral regions: the visible spectrum, the near-infrared (NIR) region, and selected mid-infrared bands. Each region offers distinct advantages and trade-offs in terms of atmospheric transmission, component technology, background noise levels, and safety constraints [3], [12].

II.2.1.2.a The main bands

- **The First Window (780–850 nm):** Historically, this window was the first to be exploited due to the maturity of AlGaAs lasers and silicon photodetectors developed for the CD/DVD industry. Although cost-effective, its performance is limited by significant Mie scattering in fog and lower eye-safety thresholds [17]. It performs adequately in clear conditions; however, water vapor absorption begins to increase at the upper edge of the band.
- **The Second Window (1300–1400 nm):** This window leverages the ecosystem of 1310 nm fiber-optic components. It offers greater resilience to aerosol scattering than the 850 nm band and corresponds to a region of reduced water vapor absorption. However, the band is narrow and situated between two strong absorption bands, meaning that any wavelength drift caused by temperature or humidity variations can lead to severe signal attenuation [9].
- **The Third Window (1500–1600 nm):** The current industry standard, centered at 1550 nm, provides the most favorable balance of performance and safety. It exhibits excellent atmospheric transmission with losses below 0.2 dB/km and utilizes high-performance C-band telecommunications hardware, including Erbium-Doped Fiber Amplifiers (EDFAs) [9]. Most importantly, its eye-safety threshold is approximately 50 times higher than at 850 nm, thereby permitting the higher power levels necessary for long-distance, high-capacity links [6], [10].

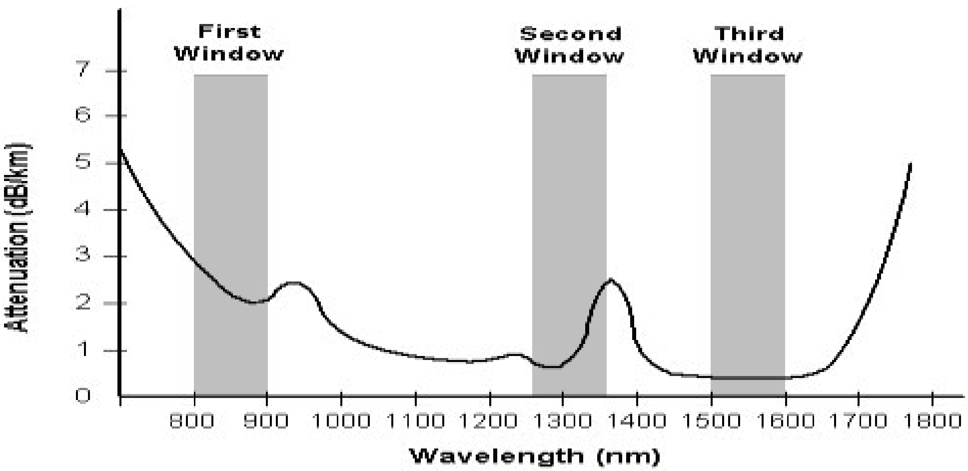

Figure II.1: Optical Frequency low attenuation Bands.

II.2.1.2.b The special bands

Beyond the three standard near-infrared (NIR) windows, several additional regions of the electromagnetic spectrum are employed for specialized Free-Space Optical applications. These are selected primarily to overcome specific atmospheric challenges or to enable non-traditional communication links [8].

- **Mid-Infrared Windows (3–5 µm)**

This region represents a key research area utilizing Quantum Cascade Lasers (QCLs). These wavelengths offer reduced molecular absorption and improved performance in haze relative to standard NIR bands. However, the requirement for specialized detectors and the high component costs currently restrict their use to military and high-end research applications [8].

- **Long-Wave Infrared Window (8–12 µm)**

Known as the "thermal" window, this region is the most effective at penetrating heavy fog, smoke, and dust because it is significantly less affected by Mie scattering [3]. Although well-suited for all-weather performance, it typically requires bulky CO_2 lasers and lacks the high-speed component ecosystem available in the telecommunications bands.

- **Visible Light Communication (400–700 nm)**

Commonly referred to as VLC or Li-Fi, this band serves as the standard for indoor high-speed networking. Outdoor deployment is limited to very short distances or signaling applications (e.g., vehicle-to-infrastructure communication) because it is highly susceptible to solar interference and intense atmospheric scattering [6].

- **Ultraviolet Band (200–280 nm)**

The "Solar-Blind" region is characterized by nearly zero background noise, as the ozone layer absorbs solar UV radiation. Its unique advantage is Non-Line-of-Sight (NLOS) communication: strong atmospheric scattering allows the signal to reach a receiver even when obstacles block the direct path. The trade-off is a very high attenuation rate, restricting the range to under 1 km [8].

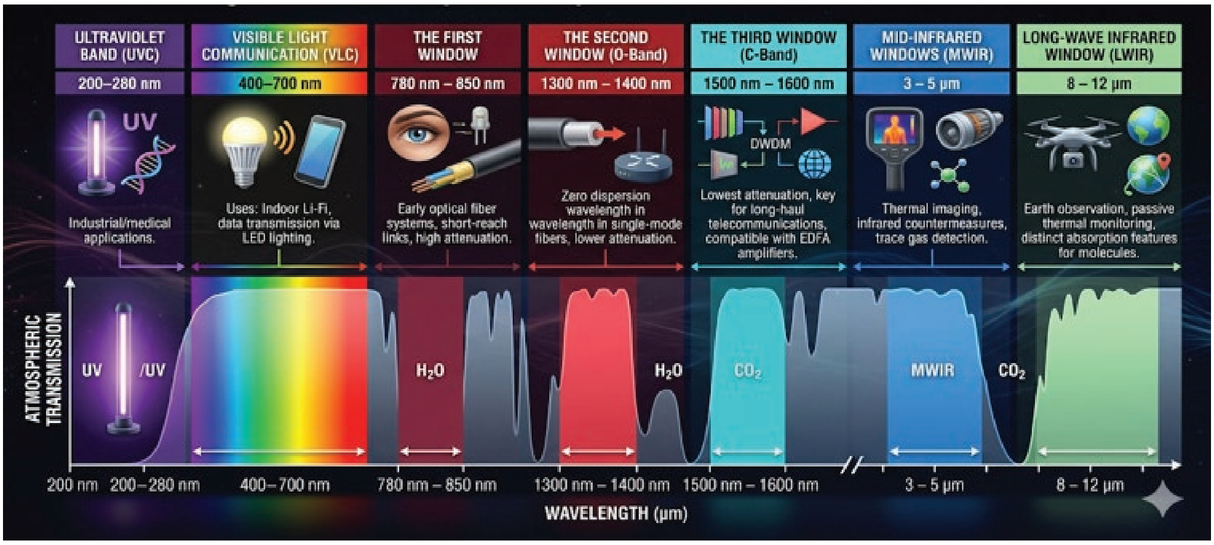

Figure II.2: Optical Frequency Bands and application.[27]

II.2.1.3 Advantages of optical frequencies

Operating at optical frequencies in the range of 200 to 400 THz provides several advantages over traditional Radio Frequency (RF) systems [4], [10]:

- ✓ **Enormous Bandwidth:** High carrier frequencies support massive data rates (10 Gbps to 100+ Gbps) and enable Wavelength Division Multiplexing (WDM), whereby multiple data streams are packed into a single optical link.
- ✓ **License-Free Spectrum:** Unlike RF, the optical spectrum remains unregulated worldwide, allowing links to be deployed without expensive licensing or frequency coordination [4].
- ✓ **Immunity to Electromagnetic Interference:** Optical signals do not interact with radio waves. FSO links are therefore completely immune to electromagnetic interference from power lines, cellular towers, or lightning discharges [17].

II.2.2 Basic Concepts of Light Propagation

The transmission of information using light is governed by the fundamental principles of wave optics. Unlike traditional radio waves, optical signals operate at much higher frequencies, offering substantial bandwidth but necessitating a precise understanding of how light interacts with its environment [16].

II.2.2.1 Diffraction

When light passes through an aperture or around an obstacle, it does not simply cast a sharp geometric shadow. Instead, it undergoes diffraction—a phenomenon in which the wavefront spreads into the shadow region. In high-speed optical systems, diffraction constitutes a primary factor in signal loss and beam spreading [7], [16].

II.2.2.1.a Huygens-Fresnel Principle

The Huygens-Fresnel principle posits that every point on a wavefront serves as a source of secondary spherical wavelets. The resulting wavefront at any subsequent moment is the superposition of these wavelets, which explains why light bends around edges and spreads when passing through apertures [7].

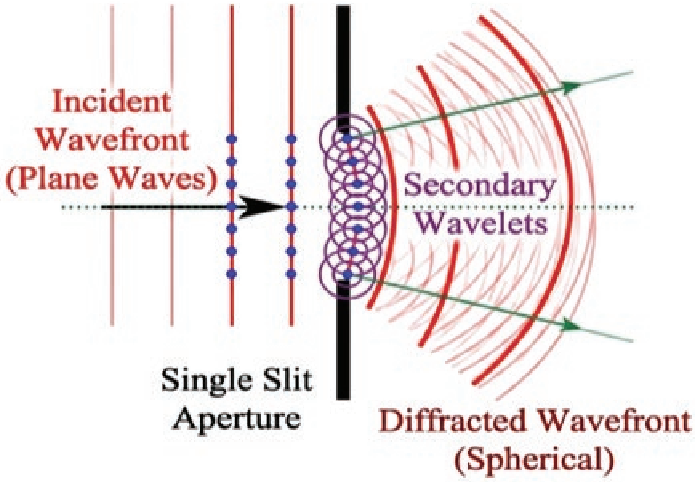

Figure II.3: HUYGENS' PRINCIPLE

II.2.2.1.b Diffraction-Limited Beam Divergence

Even an ideal laser beam undergoes natural angular spreading as it propagates—a phenomenon termed diffraction-limited beam divergence. This represents the absolute physical minimum of beam spreading permitted by the laws of physics and occurs even in the absence of atmospheric interference. Because the exit aperture of a laser acts as a finite diffracting aperture, it produces a central intensity peak known as an Airy disk, which determines the fraction of optical power that reaches a distant receiver [16].

II.2.2.1.c Role of Aperture Size

The diameter of the transmitting aperture D is the most significant factor governing beam spread. An inverse relationship exists between aperture size and the angular divergence θ, described by $\theta \propto \lambda/D$. A larger aperture therefore produces a tighter, more collimated beam, which is why long-range systems necessitate larger lenses to maintain adequate signal strength over distances of several kilometers [1], [14].θ$\theta \approx 1.22\,\lambda/D$

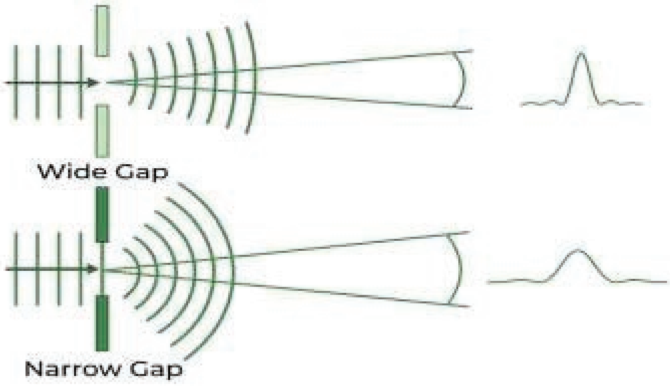

Figure II.5: role of aperture size

II.2.2.2 Interference

Interference is the phenomenon that arises when two or more light waves overlap in the same region of space. Since light behaves as an electromagnetic wave, the total intensity at any point is determined by the superposition of the individual wave amplitudes, which may either reinforce or cancel one another [7], [16].

II.2.2.2.a Coherent vs. incoherent light

For stable interference patterns to form, the light sources must be coherent, meaning they maintain a constant phase relationship over time. Lasers are highly coherent, which enables them to produce distinct interference effects that are critical for sensing and communication applications. In contrast, incoherent light from sources such as the sun or incandescent bulbs consists of many independent wave packets with random phases. Although these waves still interfere, the patterns fluctuate so rapidly that detectors perceive only a constant, averaged intensity [16] this concept is illustrated in the figure II.6 blow.

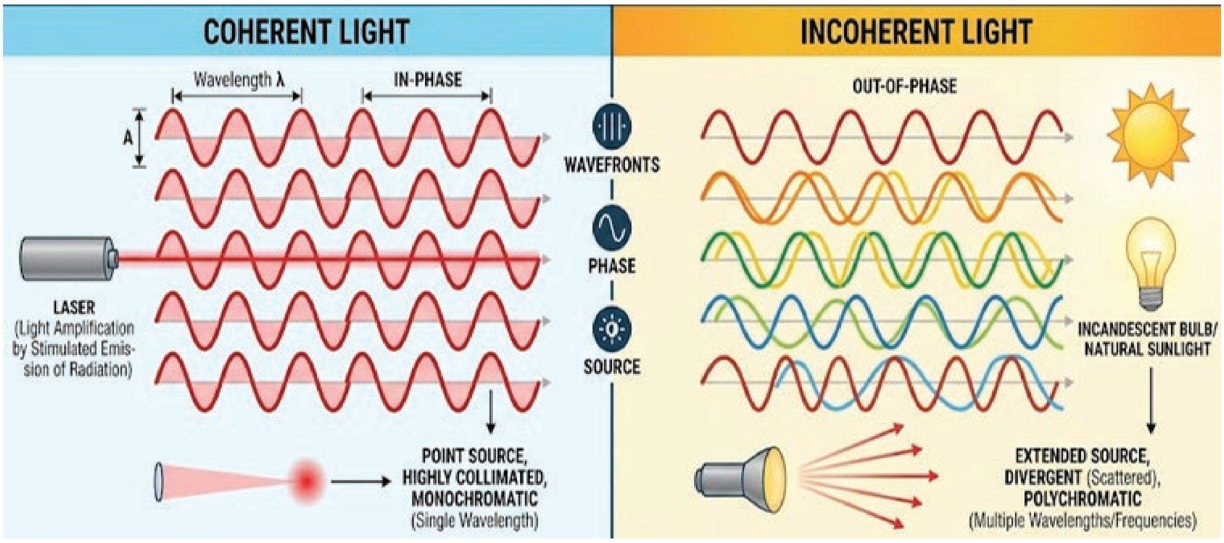

Figure II.6:coherent vs incoherent light.[27]

II.2.2.2.b constructive/destructive interference effects

The outcome of interference depends entirely on the relative phase between the interacting waves. Constructive interference occurs when the peaks and troughs of two waves are perfectly aligned (in phase), causing their amplitudes to sum and produce a region of enhanced intensity or signal strength. Conversely, destructive interference occurs when the peak of one wave aligns with the trough of another (180° out of phase), resulting in cancellation and a reduction in intensity or signal loss [7], [16].

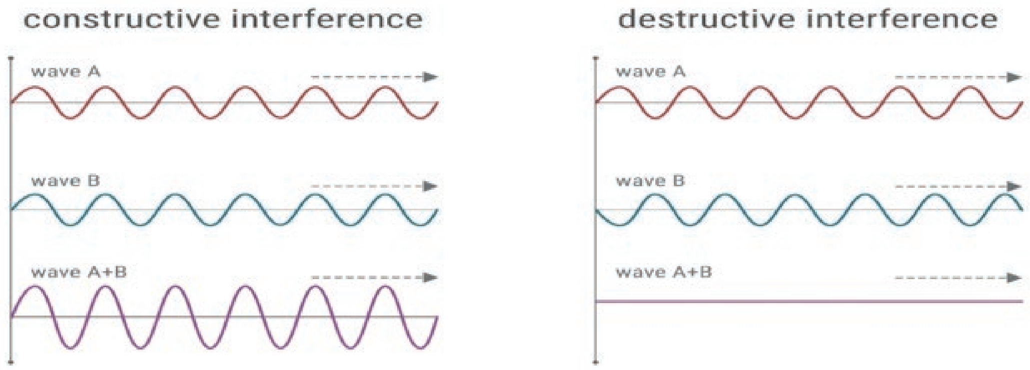

Figure II.7: Constructive interference and destructive interference

II.2.2.3 Coherence

Coherence defines the degree of correlation between the phases of a light wave, determining how well the wave maintains its phase relationship as it propagates. For a laser to function as a reliable information carrier, it must sustain a predictable phase relationship over both time and space. This orderly characteristic is the fundamental property that distinguishes laser light from thermal light, enabling the transmission of complex data across vast distances without the signal degenerating into random noise [14], [16].

II.2.2.3.a Temporal Coherence and Spectral Linewidth

Temporal coherence describes the ability of a light source to maintain a consistent phase over a specific duration. This property is inversely proportional to the spectral linewidth of the laser: a source with narrower linewidth (higher color purity) exhibits higher temporal coherence. In high-speed optical systems, maintaining high temporal coherence is critical to ensuring that the phase information of the signal remains stable and does not degrade as the wave propagates, a requirement for advanced modulation techniques [14].

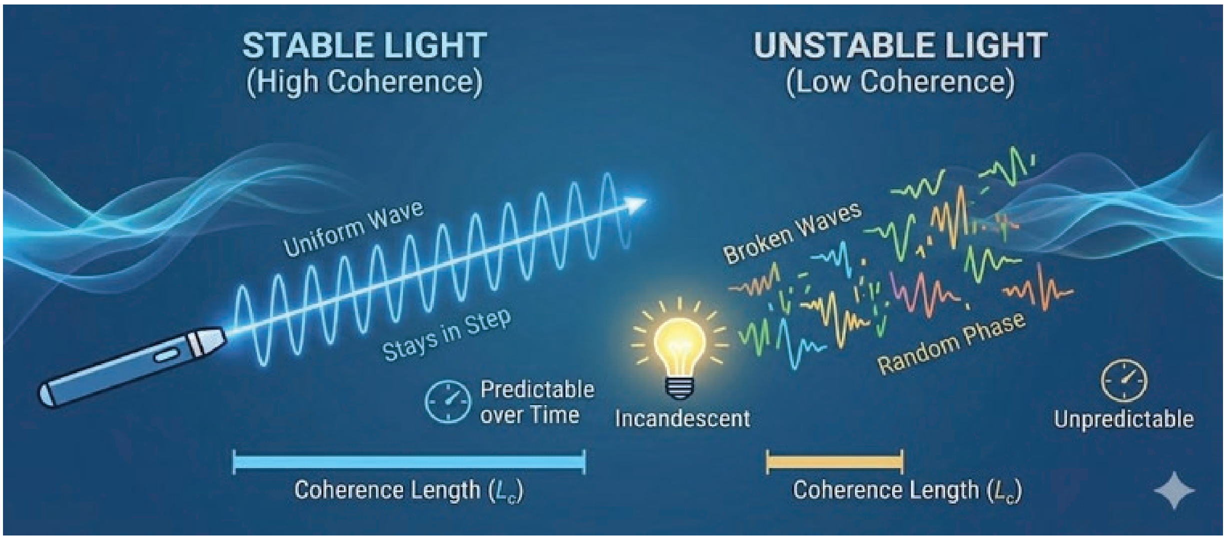

Figure II.8: *Temporal Coherence.*[27]

II.2.2.3.b Spatial Coherence and Beam Uniformity

Spatial coherence refers as shwing in the Figure II.8 to the phase correlation between different points across the transverse cross-section of the light beam. High spatial coherence indicates a uniform wavefront, with all points across the beam's width oscillating in phase.This uniformity is what enables a laser to maintain a tight, collimated beam over long distances and to be focused to a iffraction-limited spot. Without sufficient spatial coherence, a beam would rapidly lose its structural integrity an intensity, rendering it ineffective for point-to-point communication [16].

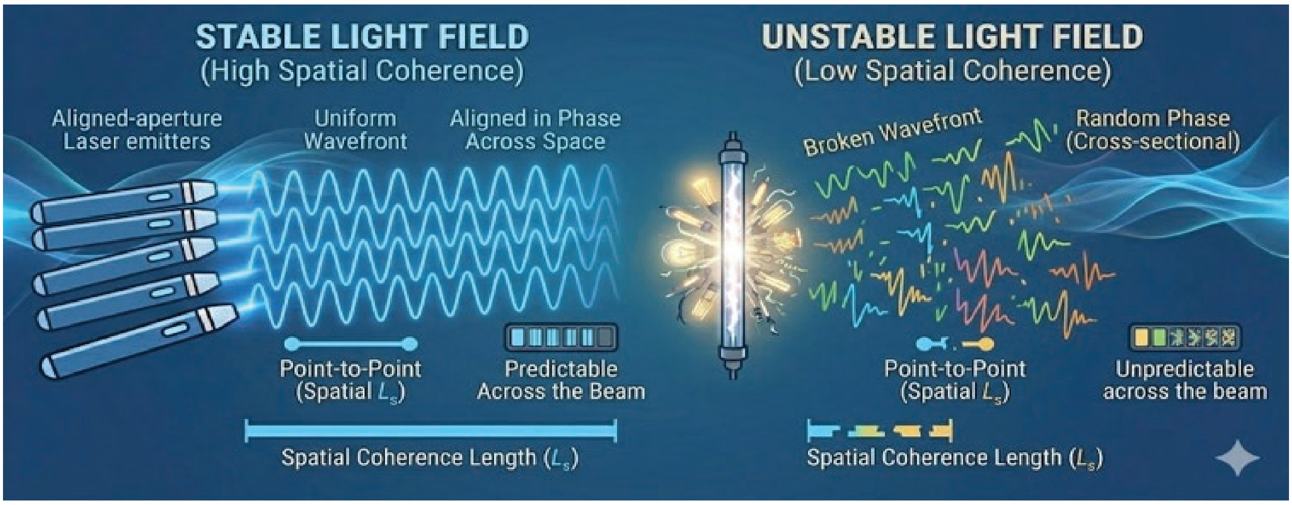

Figure II.9: *Spatial Coherence.[27]*

II.2.3 Gaussian Beam Propagation

The Gaussian beam represents as showing in the Figure II.9 the fundamental transverse electromagnetic mode (TEM_{00}) of laser propagation. A physical Gaussian beam is governed by diffraction and does not remain perfectly collimated; rather, it is defined by its unique ability to maintain its mathematical intensity profile while undergoing natural angular divergence as it propagates through space [1], [16]. The Gaussian beam is characterized by the following properties.

II.2.3.1 Beam waist & Rayleigh range

Every Gaussian beam possesses a point of minimum diameter known as the beam waist W_0, at which the wavefront is perfectly planar. The behavior of the beam in the vicinity of this waist is governed by the Rayleigh range Z_R, defined as the distance from the waist to the point at which the beam's cross-sectional area has doubled [1], [7].

$$Z_R = \frac{\pi {W_0}^2}{\lambda} \quad \textbf{(2.1)}$$

Within the Rayleigh range, the beam remains relatively collimated and propagates as an approximately parallel cylinder of light. Beyond the Rayleigh range, the beam enters the far-field region, where it begins to diverge linearly, assuming a conical profile [16].

II.2.3.2 Divergence

As a Gaussian beam propagates away from the beam waist, it undergoes angular divergence—a gradual expansion of the beam radius. This divergence is intrinsically linked to the wavelength λ and the waist size W_0, with a smaller initial focus resulting in more rapid far-field spreading. The divergence angle θ is given by $\theta = \lambda/(\pi W_0)$ [1], [14].λ

$$D = \frac{\lambda}{\pi W_0} \quad \textbf{(2.2)}$$

II.2.3.3 Geometric Losses

Geometric losses represent the reduction in optical power caused by the physical spreading of the laser beam as it propagates from the transmitter to the receiver. In any long-range optical link, the beam eventually expands to a diameter exceeding that of the receiving aperture, meaning that only a fraction of the transmitted energy is successfully collected [1], [12].

II.2.3.4 Impact of beam divergence on link alignment and pointing losses.

Beam divergence directly determines the difficulty of link alignment and the severity of pointing losses. A narrow beam (low divergence) delivers higher power density to the receiver but demands extreme precision, as even a small angular misalignment can displace the receiver from the high-intensity beam center into the weaker periphery of the Gaussian profile. This sensitivity implies that environmental factors such as mechanical vibration or atmospheric effects can induce significant signal fading [1], [12]. To mitigate this effect, system design must strike a balance: a slightly wider beam simplifies alignment and reduces pointing losses at the expense of received power density.

II.3 Atmospheric Effects on Optical Signal

The performance of Free-Space Optical communication systems is fundamentally limited by the atmosphere, which acts as a dynamic and often unpredictable transmission medium [1], [5]. Unlike optical fiber, wherein the signal is protected within a glass core, FSO signals are exposed to the complex physical chemistry and fluid dynamics of the air. This section examines the three primary atmospheric challenges: the permanent loss of signal through attenuation, the temporal and spatial distortions caused by turbulence, and the operational limitations imposed by adverse weather conditions.

II.3.1 Atmospheric Attenuation

II.3.1.1 Absorption by Atmospheric Gases

Atmospheric absorption occurs when gas molecules primarily water vapor (H_2O), carbon dioxide (CO_2), and ozone (O_3) absorb photons at specific wavelengths and convert their energy into heat. This process is highly wavelength-dependent and gives rise to opaque spectral regions where communication is impractical. To maintain signal integrity, FSO systems are designed to operate in spectral bands where absorption is minimal and the atmosphere remains relatively transparent [3], [5].

II.3.1.2 Scattering Mechanisms

Scattering refers to the redirection of optical energy away from its intended propagation path, as distinct from absorption, which converts the energy to heat. Scattering is categorized into two principal types [13]:

Rayleigh scattering: Caused by particles and molecules much smaller than the wavelength of light. This scattering mechanism is more pronounced at shorter wavelengths.

Mie scattering: Caused by larger aerosols such as dust, smoke, and haze, whose dimensions are comparable to the wavelength. In the infrared spectrum typically employed for FSO, Mie scattering constitutes the dominant attenuation mechanism, as the size of common atmospheric particles often matches the signal wavelength [3], [13].

II.3.2.3 Kim's law

In the domain of Free-Space Optical (FSO) communications, Kim's law provides a critical empirical framework for quantifying atmospheric attenuation, specifically addressing the severe signal degradation caused by Mie scattering under dense fog and low-visibility conditions. Expanding upon the foundational Kruse model, Kim refined the calculation of the specific attenuation coefficient by introducing a piecewise, visibility-dependent function for the scattering particle size distribution parameter, q. The model dictates the attenuation coefficient as:

$$ß = \frac{3.91}{V}\left(\frac{\lambda}{550}\right)^{-q} \quad \textbf{(2.3)}$$

where V represents the atmospheric visibility in kilometers and lambda denotes the operational wavelength in nanometers. Kim's pivotal theoretical contribution was recognizing that at extremely low visibilities specifically when V drops below 0.5 kilometers optical attenuation becomes entirely independent of the transmission wavelength, rendering q = 0. This nonlinear mathematical adjustment is indispensable for accurately calculating complex link budgets and ensuring the reliability of high capacity Wavelength Division Multiplexing (WDM) systems. By utilizing this framework, network architects can precisely predict path loss and dynamically optimize advanced modulation techniques to maintain robust data integrity despite severe tropospheric impairments.

II.2.1.4 The Beer-Lambert Law

the Beer-Lambert Law serves as the fundamental physical principle governing atmospheric transmittance and signal power degradation over a propagation medium. For unguided optical transmission, this theorem mathematically defines the relationship between the received optical power, IL, and the transmitted power, I0, through the exponential decay function:

$$I_L = I_0 \, e^{-\sigma L} \quad \textbf{(2.4)}$$

where L represents the physical link distance and σ denotes the total atmospheric extinction coefficient. This vital coefficient comprehensively aggregates both the absorption and scattering cross-sections of localized atmospheric constituents, making the mathematical law strictly indispensable for modeling severe environmental impairments. This calculation is particularly critical when characterizing the extreme signal attenuation caused by dense dust storms, airborne sand suspension, and aggressive aerosol scattering prevalent in arid desert climates and volatile meteorological environments. As optical waves propagate through these challenging mediums, particulate interference heavily disrupts both the phase and amplitude of the transmitted beam. Consequently, accurately applying the Beer-Lambert Law allows us to calculate precise link margins and establish robust, fault-tolerant power budgets. This fundamental scaling ensures that high-capacity Wavelength Division Multiplexing (WDM) optical networks can sustain reliable bit error rates and maintain an optimal optical signal-to-noise ratio, successfully operating despite intense particulate concentrations, rapid temperature fluctuations, and unpredictable tropospheric turbulence.

This relationship serves as the primary tool for link budget calculation and for determining the maximum effective range of an optical communication link [3].

II.3.2 Atmospheric Turbulence

II.3.2.1 Refractive Index Fluctuations

Atmospheric turbulence is primarily driven by temperature and pressure gradients that create localized pockets of air with varying densities, known as optical eddies [1], [24].

These eddies act as transient, moving refractive elements along the beam path, causing the air's refractive index to fluctuate randomly. As the laser beam traverses these inhomogeneous cells, different portions of the optical wavefront travel at slightly different velocities, resulting in distortion of the originally planar wavefront [1], [23].

II.3.2.2 Scintillation Effects

The physical impact of atmospheric turbulence on an optical signal manifests in three distinct ways: scintillation, beam wander, and beam spreading [1], [11]. Scintillation refers to the rapid fluctuation of received light intensity, analogous to the twinkling of stars. Beam wander occurs when large-scale eddies deflect the entire beam from its intended path, while smaller eddies cause the beam to spread beyond its theoretical diffraction limit. Collectively, these effects result in significant signal fading and reduced power density at the detector [1], [24].

II.3.2.3 Statistical Turbulence Models

Because turbulence is a stochastic process, mathematical models are employed to predict signal behavior and to design fade-protection margins [1], [12]. The log-normal distribution is typically used to model weak turbulence over short propagation distances. For more severe conditions, the gamma–gamma distribution is the standard model, as it separately accounts for the effects of both large-scale and small-scale eddies. In cases of extreme turbulence, the K-distribution is applied to accurately characterize the severe fluctuations in the received signal [1].

II.3.3 Weather Effects

II.3.3.1 Fog

Fog represents the most significant impediment to FSO link reliability, as its droplet size distribution (1 to 15 μm) directly overlaps with common optical communication wavelengths, resulting in intense Mie scattering [3], [15]. Fog is primarily classified by its formation mechanism: radiation fog, which forms due to terrestrial cooling on clear nights, and advection fog, which develops when warm, moist air moves over a colder surface. To quantify the resulting signal degradation, the Kruse model is employed to derive the attenuation coefficient as a function of visibility V [3]:

$$\beta(\lambda) = \frac{3.91}{V}\left(\frac{\lambda}{\lambda_0}\right)^{-q} \quad \textbf{(2.5)}$$

In this expression, q is a correction factor dependent on the particle size distribution. This model allows the correlation of standard meteorological visibility data with expected decibel loss per kilometer [15].

II.3.3.2 Rain

Rain droplets are significantly larger than the wavelength of laser light (100 to 1000 µm); consequently, rain attenuation is governed by geometric scattering rather than the intense Mie scattering observed in fog [3]. The specific attenuation is typically calculated using the power-law relationship [18]:

$$A = a \cdot R^{b} \quad \textbf{(2.6)}$$

where R denotes the rain rate in mm/h. For professional link analysis, the ITU-R P.838-3 model provides the standard coefficients for predicting rain-induced attenuation [18]. Although typically less severe than fog, heavy precipitation can still induce significant signal fading that must be accounted for in the system power margin.

II.3.3.3 Snow

Snow presents a complex atmospheric challenge due to the structural diversity of snowflakes and their varying moisture content [3]. Attenuation is categorized by the physical state of the precipitation: dry snow, which acts primarily as a crystalline scatterer with relatively low extinction, and wet snow, which features larger, stickier flakes that cause substantially higher signal loss [5]. Because snowflakes lack a uniform spherical geometry, empirical models such as the Marshall–Palmer snowflake size distribution are employed to estimate the extinction cross-section and its impact on the optical path.

Beyond atmospheric scattering, snow poses a significant mechanical risk to link availability. Unlike rain, which naturally drains from surfaces, wet snow can accumulate on the transceiver's optical aperture, leading to complete physical blockage of the signal [17].

While atmospheric attenuation and weather define the physical limits of the propagation medium, overcoming these constraints requires a transition from reliance on raw transmission power to sophisticated signal processing. By employing advanced modulation techniques, systems can encode significantly more information per photon while enhancing resilience to atmospheric fading [6], [10]. These techniques allow the link to dynamically optimize performance, maximizing data rates under clear conditions and maintaining connectivity during periods of severe atmospheric interference.

II.3.3.4 Dust

In Free-Space Optical systems, airborne dust degrades signals primarily through Mie scattering, which occurs because dust particle sizes are comparable to standard FSO laser wavelengths (780–1600 nm) [5]. This signal attenuation is quantified by the Beer–Lambert law, which yields the total attenuation coefficient. Using observable meteorological data, the Koschmieder law is applied [3]:

$$V = \frac{-\ln(0.02)}{\sigma} \quad \textbf{(2.7)}$$

which relates the extinction coefficient directly to atmospheric visibility V.

II. 4 Advanced Modulation Techniques

To effectively address the challenges of the atmospheric channel, optical communication systems employ two distinct architectural approaches for signal recovery: direct detection and coherent detection. The choice between them represents a fundamental trade-off between hardware simplicity and the capacity to maintain high data rates over long, turbulent propagation paths [6], [10].

Direct Detection and **Coherent Detection**. The choice between them represents a fundamental trade-off between hardware simplicity and the ability to maintain high data rates over long, turbulent distances.

II. 4.1 Non-Coherent (Direct Detection)

Direct detection is the most widely deployed architecture in FSO systems due to its cost-effectiveness and architectural simplicity [6]. In this configuration, the receiver consists of a photodetector that converts the incoming optical power directly into an electrical current, effectively measuring the envelope of the signal while disregarding the carrier phase and frequency. The most common variants are described below.

II. 4.1.1 On-Off Keying (OOK)

On–Off Keying (OOK) serves as the fundamental baseline for FSO communication owing to its inherent simplicity and low-cost implementation [6], [17]. In this scheme, digital data are transmitted by modulating the intensity of the laser source: a binary "1" is represented by a pulse of light, while a binary "0" is indicated by its absence. OOK can be deployed in two primary formats: Non-Return-to-Zero (NRZ), wherein the pulse occupies the entire bit interval, and Return-to-Zero (RZ), wherein the pulse is shorter than the bit duration to conserve power and improve timing synchronization. Although its straightforward binary nature simplifies hardware design, OOK is highly susceptible to atmospheric scintillation and background noise, often necessitating significant power margins to maintain a stable connection under turbulent conditions [10].

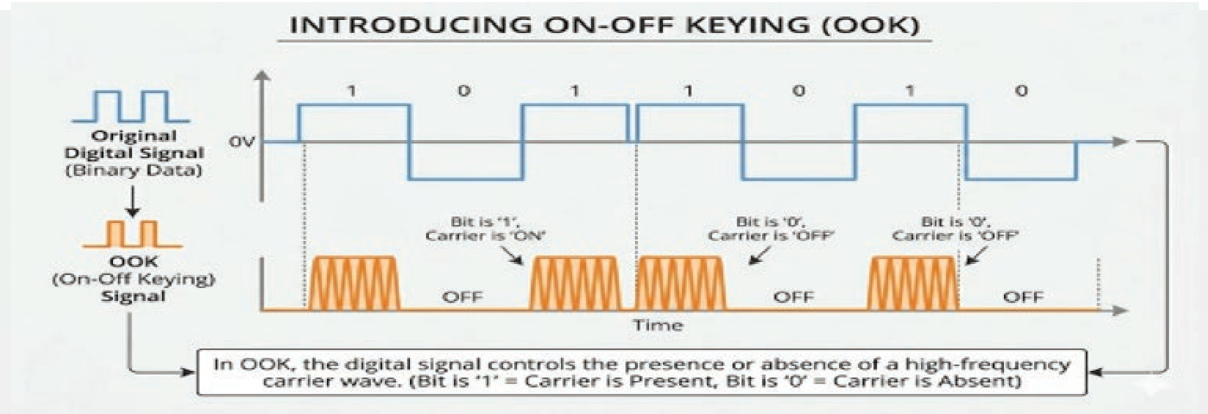

Figure II.10*: *On-Off Keying (OOK)[27]

II. 4.2 Pulse Position Modulation (PPM)

Pulse Position Modulation (PPM) is an M-ary orthogonal signaling scheme that prioritizes power efficiency over bandwidth efficiency, making it well suited for long-range or power-constrained FSO links [6], [22]. Rather than simply switching the laser on or off to represent a single bit, PPM divides a fixed time frame into M distinct time slots and transmits a single high-intensity pulse in exactly one of them; the position of that pulse encodes the decimal value of the transmitted data bits. This concentration of energy within a single slot allows the signal to penetrate atmospheric attenuation more effectively than OOK at the same average power. However, this efficiency is achieved at the cost of increased system complexity, as the receiver requires precise synchronization to identify slot boundaries, and the systemdemandssignificantly higher bandwidth to accommodate the narrow time slots required for high data rates [10].

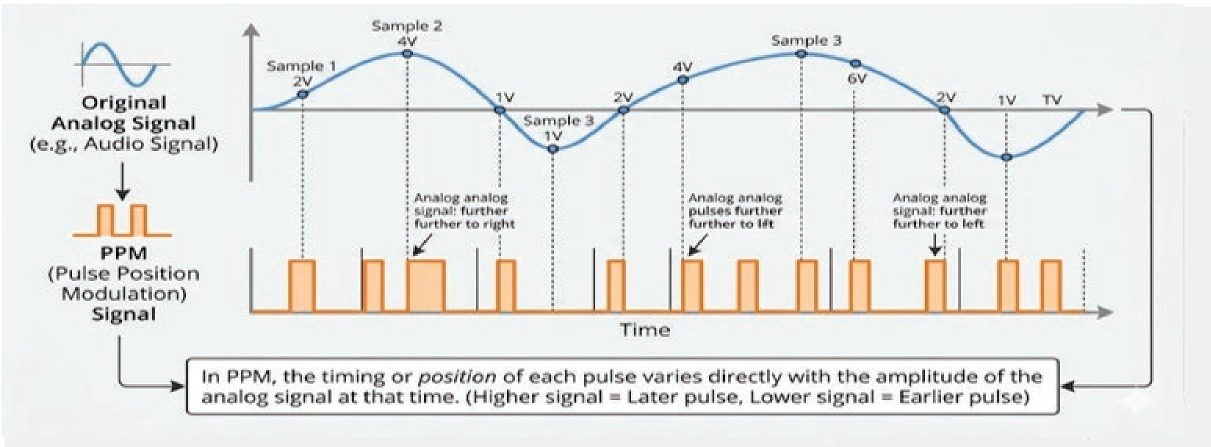

Figure II.11*: *Pulse Position Modulation (PPM)[27]

II. 4.2 Coherent Detection (Advanced Formats)

Coherent detection represents the most advanced optical communication technology, treating light as a continuous electromagnetic wave rather than a stream of discrete photons [4], [16]. By exploiting the wave-like properties of light—specifically phase, frequency, and amplitude—coherent systems achieve significantly higher data rates and superior receiver sensitivity compared with direct detection methods.

II. 4.2.1 The Coherent Architecture

The defining feature of a coherent receiver is the Local Oscillator (LO), a secondary laser located at the receiver. The incoming signal is optically mixed with the LO output, which amplifies the weak received signal and enables the receiver to extract the complete information encoded in the optical field [4]. Unlike direct detection, which measures only the signal intensity, coherent detection can discriminate between different optical phase states and can even separate data transmitted on orthogonal polarization states. Because the receiver captures the full electric field of the optical wave, digital signal processing (DSP) can be applied to compensate for the distortions introduced by atmospheric turbulence after signal reception [4], [12].

II. 4.2.2 Common Modulation Formats for Coherent Detection

Advanced modulation formats utilize the wave-like properties of light—specifically phase and amplitude—to transmit data. Unlike simple intensity-based methods, these formats require a coherent receiver architecture to accurately track and decode the complex state of the incoming optical field [4], [16].

II. 4.2.2.a Phase Shift Keying (BPSK, QPSK)

Phase Shift Keying (PSK) is a sophisticated modulation technique that encodes data by altering the phase of the optical carrier wave while maintaining a constant amplitude. This makes PSK formats inherently more resilient than intensity-based methods to the scintillation effects induced by atmospheric turbulence, as the information is encoded in the temporal phase of the wave rather than in its instantaneous intensity [4], [16].

- **Binary Phase Shift Keying (BPSK)**

BPSK is the simplest and most robust form of phase modulation, employing two distinct phase states typically 0° and 180° to represent binary 0 and 1, respectively. Because these two states are maximally separated in the phase domain, BPSK offers the highest noise immunity among all modulation formats and can maintain a reliable link even under extremely low signal-to-noise ratio (SNR) conditions [4], [22]. In professional FSO deployments, BPSK is frequently employed as a fallback or survival mode for deep-space missions or under highly turbulent atmospheric conditions, ensuring that a communication link remains active even at the cost of reduced data throughput.

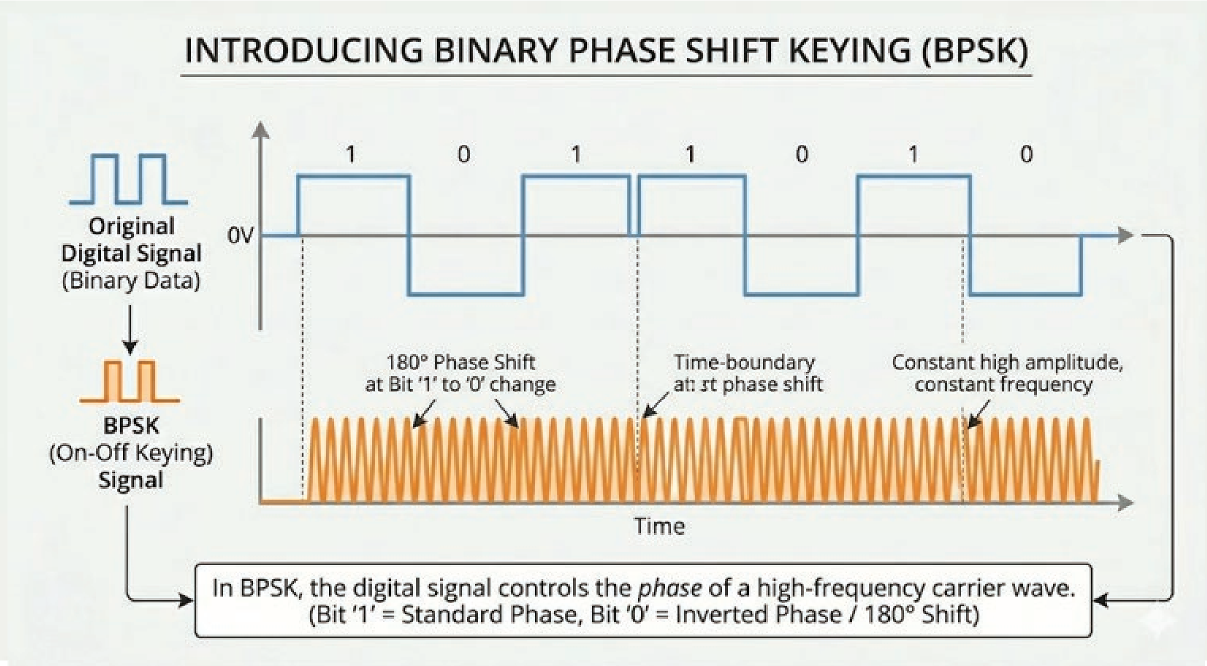

Figure *II*.12: *Binary Phase Shift Keying (BPSK)* [27]

- **Quadrature Phase Shift Keying (QPSK)**

QPSK increases spectral efficiency by employing four distinct phase shifts (45°, 135°, 225°, and 315°), allowing each symbol to represent two bits of data (00, 01, 11, 10). This configuration effectively doubles the data rate compared with BPSK without requiring additional bandwidth [4]. Although QPSK demands a more precise receiver to discriminate among the four phase states, it offers an advantageous balance between high-speed performance and atmospheric resilience and is currently the industry standard for high-bandwidth satellite-to-ground and inter-satellite laser links [8].

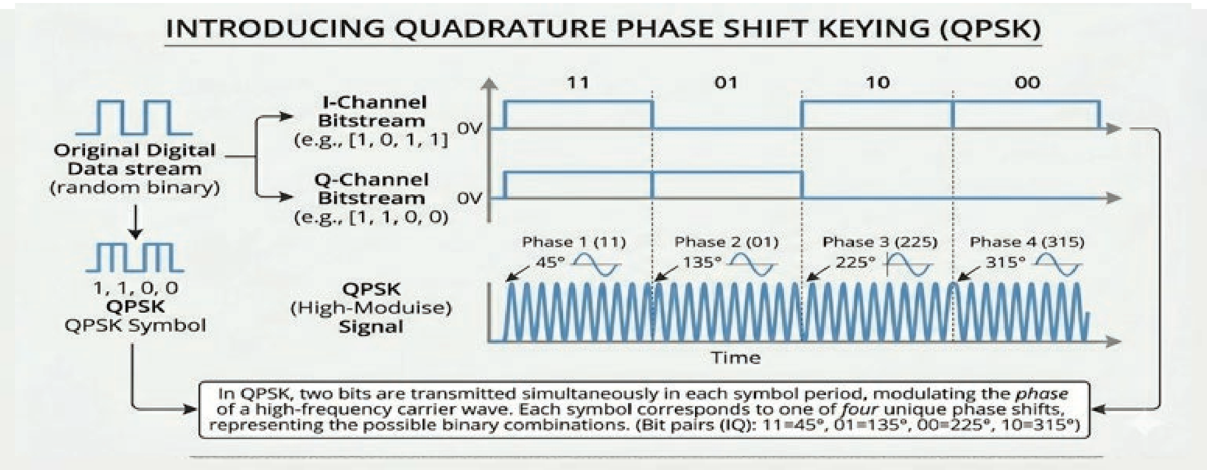

***Figure* II.*13:* Quadrature Phase Shift Keying (QPSK)** [27]

II. 4.2.2.b Differential Phase Shift Keying (DPSK)

Differential Phase Shift Keying (DPSK) is widely regarded as an advantageous compromise for free-space optical communication, bridging the gap between the simplicity of direct detection and the high performance of full coherent systems [6], [10]. In this format, digital information is encoded not in the absolute phase of the carrier wave but in the phase difference between successive pulses. For instance, a binary "0" might be represented by maintaining the same phase as the preceding pulse, while a binary "1" is represented by a 180° phase shift. The critical advantage of this approach is that the receiver does not require a complex Local Oscillator laser as a phase reference; instead, it employs a delay-line interferometer to compare each incoming pulse with a delayed replica of the previous pulse. By using the signal as its own reference, DPSK becomes exceptionally resilient to the rapid phase fluctuations and frequency offsets induced by atmospheric turbulence that would otherwise destabilize a standard coherent link. This makes DPSK an ideal choice for high-speed, long-range FSO deployments where maintaining a stable phase reference is challenging due to the dynamic nature of the outdoor propagation environment [10].

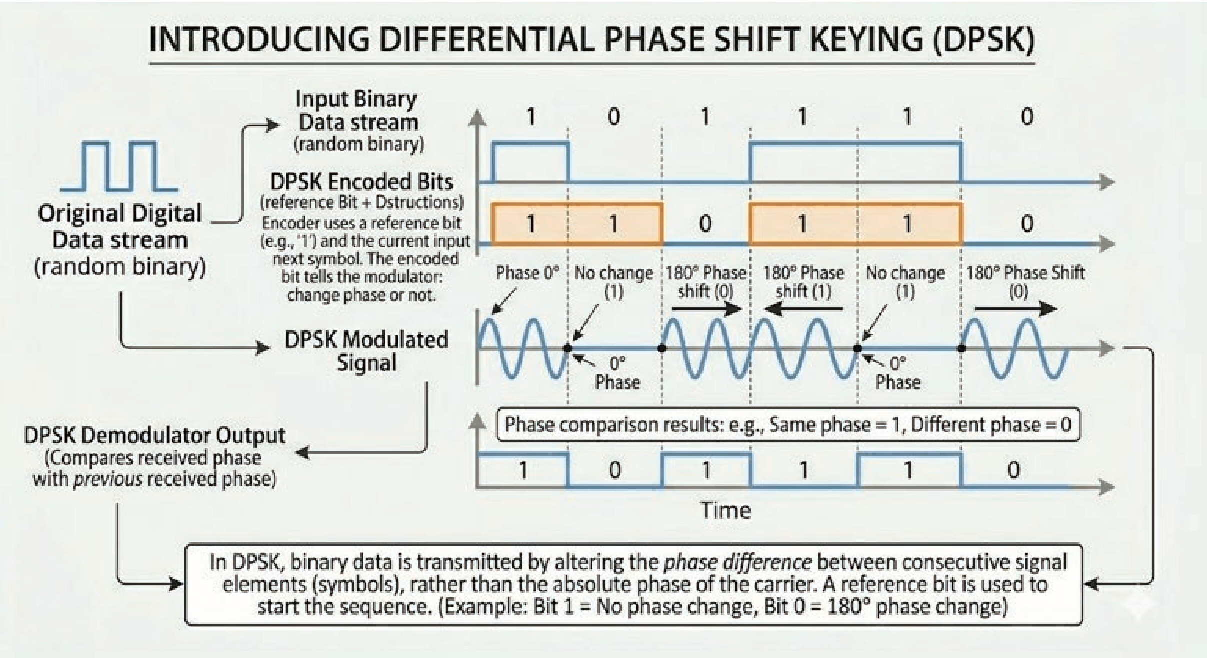

Figure *II*.14: *Differential Phase Shift Keying (DPSK)* [27]

II. 4.2.2.c Quadrature Amplitude Modulation (M-QAM)

Quadrature Amplitude Modulation (M-QAM) is the most sophisticated modulation format employed in high-capacity FSO links, offering the highest spectral efficiency by treating the optical carrier as a complex vector [4], [16]. By modulating both the amplitude (intensity) and the phase (timing) of the light wave simultaneously, M-QAM can transmit multiple bits of data within a single symbol. Unlike binary schemes that transmit only one bit per symbol, M-QAM employs a grid-like constellation of points; for example, 16-QAM transmits 4 bits per symbol, whereas 64-QAM transmits 6 bits per symbol. This capability enables the system to achieve throughputs reaching hundreds of gigabits per second without requiring an increase in the physical bandwidth of the laser. However, decoding these complex signals necessitates a full coherent receiver architecture with high-speed digital signal processing to accurately map the received waves onto the intended constellation. While M-QAM represents the standard for high-speed performance, it is also the most sensitive to atmospheric impairments: because the constellation points are densely packed, even minor scintillation or phase noise can degrade signal quality, making this format best suited for clear-sky conditions or systems incorporating adaptive optics [4], [12].

II. 5 CONCLUSION

Free-Space Optical systems' performance is essentially governed by random features of the atmospheric channel. The broad bandwidth of near-infrared windows, however, link reliability is not clear owing to environmental stressors such as aerosol absorption, turbulence fading and severe weather. To conquer these physical constraints, it is necessary to redirect from increasing the raw transmission power to new modulation formats. By moving from simple direct-detection schemes (OOK, PPM) to high-order coherent schemes (PSK, M-QAM), modern FSO systems can better tackle atmospheric distortions for reliable and high-capacity connectivity needed for next-generation optical wireless networks.

Chapter III

Advanced Modulation Techniques

for WDM-FSO system

III.1 Introduction

Recent advances in Wavelength Division Multiplexing have positioned Free-Space Optical (WDM-FSO) communication as a scalable solution for next-generation wireless backhaul, with reported aggregate capacities spanning 40 Gbps in tropical 16-channel prototypes [1], 60 Gbps in 8 × 7.5 Gbps C-band links [2], and 1.28 Tbps in 32 × 40 Gbps DWDM-FSO confgurations [3], [4]. Earlier experimental milestones such as 4 × 10 Gbps over 1.2 km [5] and 8 × 10 Gbps over 3.4 km with an optical repeater [6],further validate the maturity of the technology. However, the deployment envelope of such high-capacity links is fundamentally constrained by the atmospheric channel [7], with the desert and arid belts of the Sahara ,the Arabian Peninsula, and the Middle East representing some of the most challenging environments owing to the combined action of visibility-limited dust/sand scattering [8], intense solar loading, and steep refractive-index gradients [9]. Recent feld driven and simulation based studies in these regions [10],[11] have demonstrated that dust-driven attenuation and thermal turbulence can each reduce reliable link reach to 1–2 km, while parallel work has shown that WDM-FSO reach in heavy rain can drop to as little as 1.2 km [12]. The modulation-format literature consistently reports that lower-order schemes NRZ-OOK, 4QAM, and pulse-position modulation (PPM) exhibit superior resilience to scintillation-induced fading compared with higher-order formats such as 16 QAM [13] [15]. Despite this body of work, the prevailing literature analyses these stressors in isolation, with most studies focused on a single impairment such as rain, fog, haze, or weak thermal turbulence [16], leaving the joint, simultaneous effect of severe sandstorm scattering and high thermal-induced turbulence on a WDM-FSO architecture as an essentially unaddressed gap one that is critical for the realistic design of high-capacity backhaul links across desert corridors.

This chapter provides a comprehensive performance evaluation of the 112 Gbps DP-16QAM FSO system and 112 Gbps DP-QPSK FSO system through a series of rigorous numerical simulations, with a focus on analyzing the atmospheric interference and turbulence characteristic of the El Oued climate. Furthermore, the impact of atmospheric attenuation on key performance indicators including BER, Q-factor, and Eye Diagram integrity will be examined to provide a clear perspective on the feasibility of deploying such systems in desert environments.

III.2 General WDM-FSO System Architecture

Wavelength-Division Multiplexing Free-Space Optics represents a hybrid, high-capacity communication paradigm that synergizes the massive spectral efficiency of optical fiber WDM with the spatial flexibility of unguided optical transmission. By simultaneously transmitting multiple distinct optical carriers through the atmosphere, WDM-FSO dramatically scales link capacity, effectively supporting data rates of 100 Gb/s and beyond without the infrastructural cost of deploying physical fiber. This architecture is pivotal for bridging the last mile access gap, providing high-bandwidth backhaul, and establishing rapidly deployable, secure communication links. The system is fundamentally delineated into three interacting sub-systems: the transmitter, the atmospheric propagation channel, and the receiver.

III.2.1 Transmitter Architecture

The transmitter architecture is responsible for generating, modulating, and spatially directing the multi-wavelength optical signal. A tightly spaced array of laser diodes generates independent optical carriers, typically operating within the 1550 nm transmission window to mitigate atmospheric absorption. Each carrier undergoes electro-optic modulation to encode high-speed digital data frequently utilizing advanced modulation formats such as Pulse Position Modulation (PPM) for power efficiency or Quadrature Amplitude Modulation (QAM) for enhanced spectral density. The precise configuration of guard bits and symbol framing is critical at this stage to maintain signal integrity at extreme bit rates. Following modulation, the independent channels are aggregated using an optical multiplexer, optically boosted and finally passed through a transmitting telescope. This optical antenna system precisely collimates the multiplexed beam to minimize divergence as it is launched into the unguided free-space medium.

III.2.2 The Atmospheric Channel

The unguided atmospheric channel acts as the propagation medium and is the primary source of signal degradation in an FSO link. As the collimated optical beam traverses this channel, it is subjected to severe optical attenuation and phase distortion. The total path loss is mathematically governed by the Beer-Lambert Law. Furthermore, optical propagation is heavily impaired by atmospheric turbulence localized fluctuations in temperature and pressure that continuously alter the refractive index of the air. This turbulence induces scintillation and beam wander, fundamentally compromising link availability and necessitating rigorous performance modeling across varying weather states and operational ranges.

III.2.3 The Receiver Architecture

The receiver architecture is engineered to capture the spatially distorted optical field, isolate the individual wavelength channels, and accurately recover the encoded data streams. An optical receiving telescope, characterized by a specific aperture size and focal length, collects the attenuated incoming wavefront and couples it into an optical fiber or directly onto a detector plane. Following optical pre-amplification to elevate the signal-to-noise ratio, the composite beam is passed through a demultiplexer to separate the constituent wavelengths. These individual optical channels are then directed into high-sensitivity photodetectors, for optical-to-electrical conversion. The final stage involves sophisticated Digital Signal Processing (DSP) to compensate for channel-induced dispersion, optimize constellation diagram clarity, and execute decision algorithms to accurately reconstruct the original bit stream despite the severe impairments introduced by the atmospheric channel.

III.3 8 channel DP-16 QAM WDM FSO System Simulation Setup

This section details the simulation environment established for a high-capacity, 8-channel DP-16QAM WDM-FSO communication link. Designed to support a data rate of 112 Gb/s per channel, the framework rigorously models the multiplexed optical architecture against the real-world, desert atmospheric dynamics specific to El Oued, Algeria. The system's performance is analyzed utilizing OptiSystem 23, an advanced optical engineering platform that enables highly accurate modeling of wavelength aggregation, dual-polarization states, and the sophisticated coherent detection processes required for multi-channel propagation.

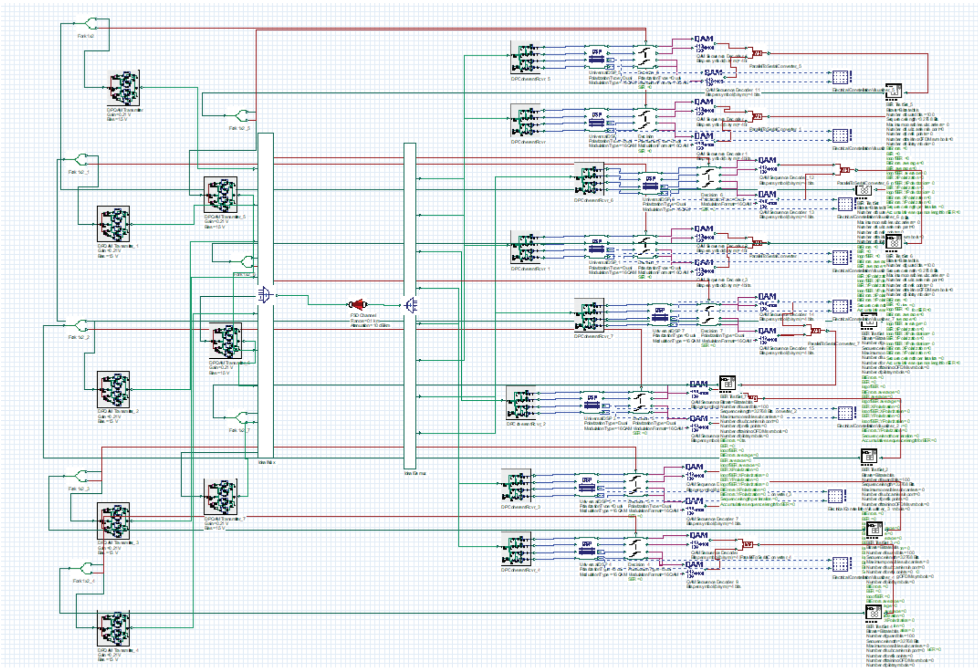

Figure 3.1 : *8 channel FSO DP-16-QAM Modulation System.*

III.3.1 The transmitter architecture of an 8-channel DP-16QAM WDM-FSO (TX)

The transmitter functions as a high-capacity optical hub that aggregates independent data streams into a single, robust beam for atmospheric transmission. It begins with an array of eight CW lasers aligned to the ITU-T C-band grid, where each wavelength serves as an independent carrier to facilitate dense wavelength multiplexing. Each channel undergoes sophisticated DP-16QAM modulation: the electrical data is mapped onto a 16-QAM constellation and processed by a Polarization Beam Splitter (PBS) to separate the signal into orthogonal X and Y polarization components. These components are individually modulated using high-speed Mach-Zehnder Modulators (MZM) and subsequently recombined via a Polarization Beam Combiner (PBC) to effectively double the spectral efficiency. These eight independent DP-16QAM signals are then merged into a single composite optical beam using a WDM multiplexer. Finally, this aggregate signal is launched into the atmosphere via a transmit telescope that collimates the beam to minimize divergence over the transmission path.

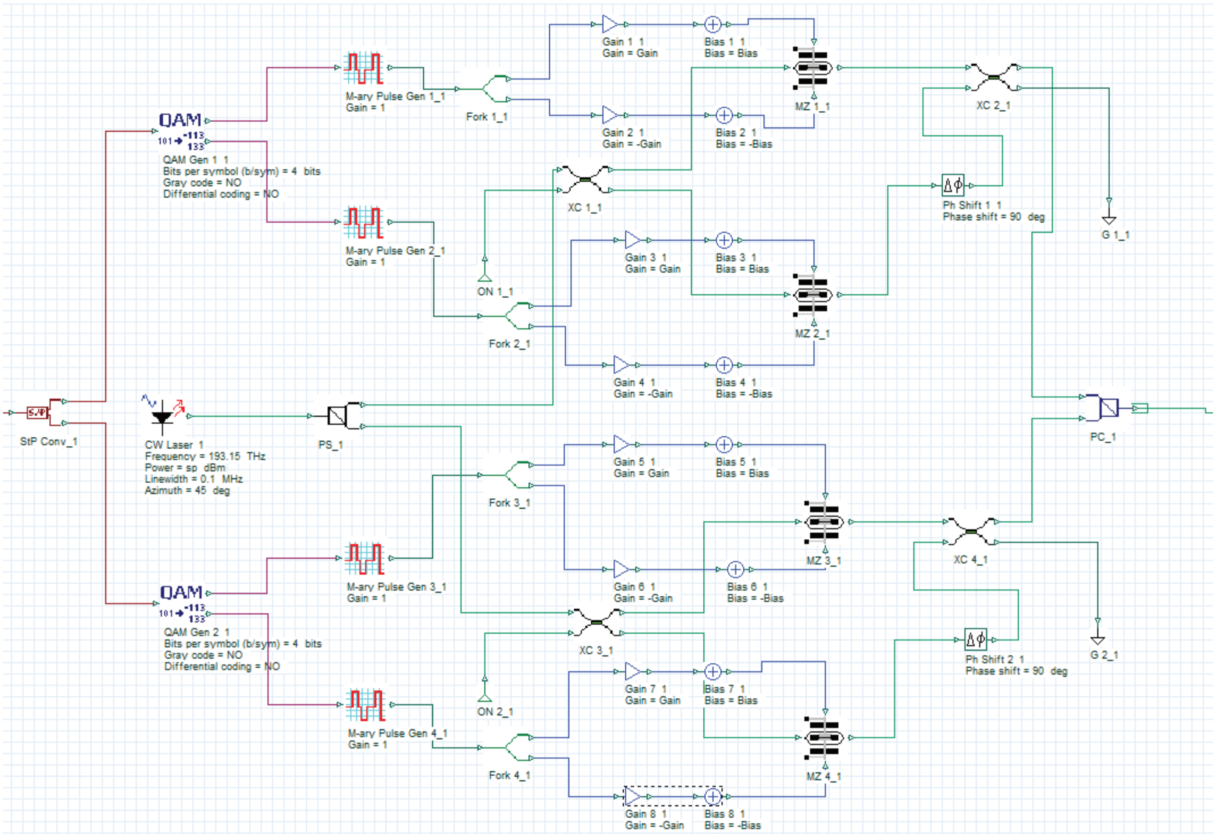

Figure* III.2: *Optical DP 16-QAM transmitter layout.

III.3.2 FSO Channel

The FSO Channel is modeled as a line-of-sight (LoS) optical link with a variable transmission range R. Atmospheric attenuation is implemented using the Beer-Lambert law. With the attenuation coefficient α varying according to five distinct weather conditions:

Clear, Light Rain, Heavy Rain, Dust Storm, and Severe Dust Storm.

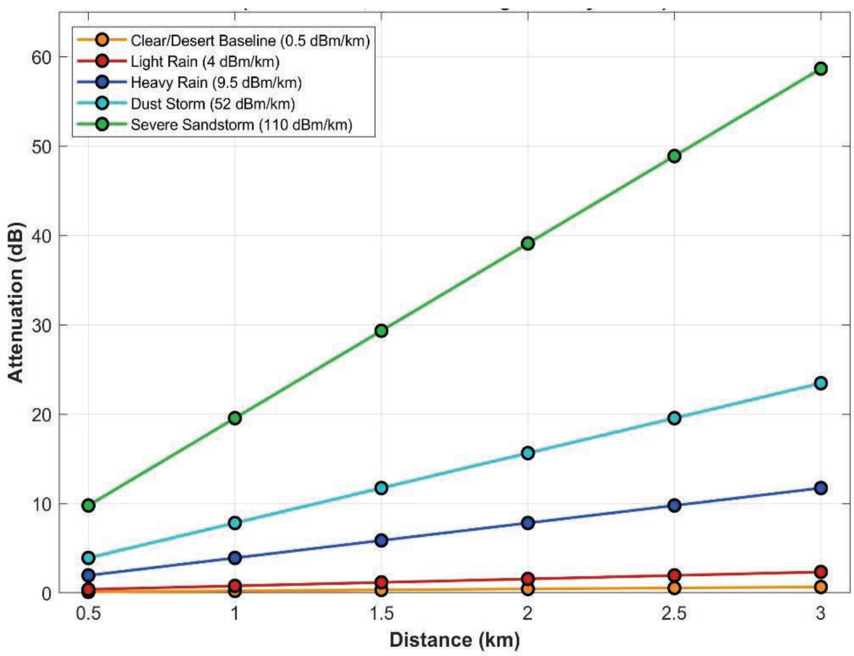

Figure III.*3 : Attenuation vs Distance under Different Weather Conditions for DP 16 QAM* .

The illustrated data provides a quantitative assessment of atmospheric-induced signal degradation, demonstrating how different weather scenarios influence the propagation efficiency over a defined distance.

III.3.3 The receiver architecture of an 8-channel DP-16QAM WDM-FSO (RX)

The receiver is engineered to perform robust coherent detection and digital signal recovery despite the severe, time-varying impairments introduced by the atmospheric propagation channel. The process initiates at the receive telescope, which captures the attenuated and distorted incoming wavefront and couples it into an optical fiber for processing. An Erbium-Doped Fiber Amplifier (EDFA) is typically utilized as a pre-amplifier to improve the optical signal-to-noise ratio (OSNR), after which a WDM demultiplexer isolates the eight individual wavelength channels. Each channel is then fed into a coherent receiver front-end, where it is mixed with a continuous-wave local oscillator (LO) laser within a 90-degree optical hybrid to extract the In-phase (I) and Quadrature (Q) components of both orthogonal polarizations. These signals are converted into the electrical domain via balanced photodetectors and subsequently digitized for sophisticated Digital Signal Processing (DSP). The DSP stage is the system's analytical core, performing essential functions including clock recovery, frequency offset estimation, polarization demultiplexing to disentangle the X and Y states, and adaptive equalization to mitigate atmospheric scintillation and phase noise, ultimately ensuring the reliable reconstruction of the high-speed 112 Gb/s per-channel data streams.

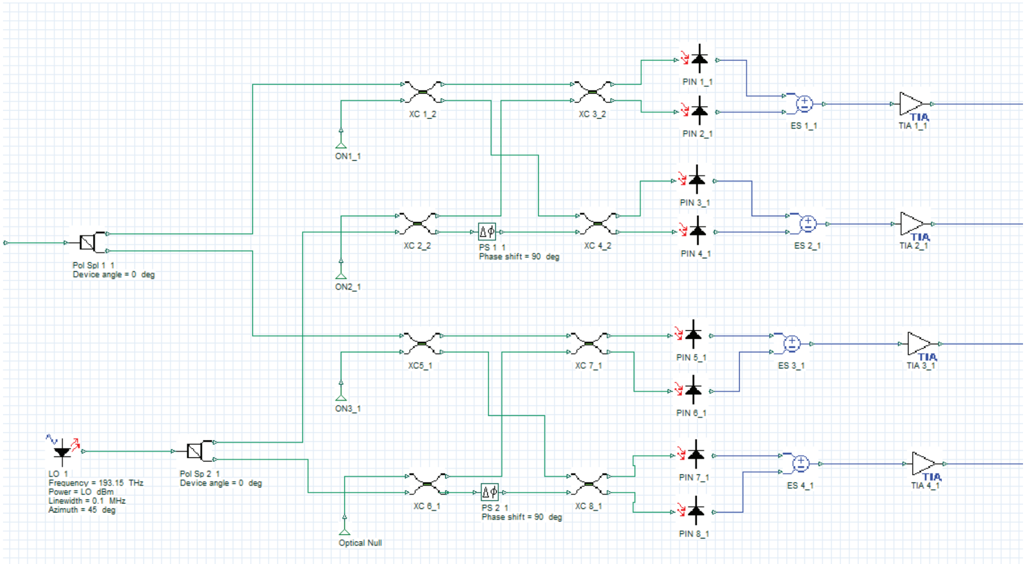

Figure III***.4:*** *Optical cohrent DP 16-QAM receiver layout.*

III.2.4 Additional Supporting Components

DSP for 16-QAM : The Digital Signal Processing (DSP) unit in a 16-QAM system acts as the brain of the receiver, responsible for recovering data from an optical signal that has been severely distorted by harsh atmospheric conditions. The process begins with normalization and resampling to stabilize the electrical signal levels. This is followed by polarization demultiplexing, a critical step in DP (Dual Polarization) systems to decouple the interference between the horizontal and vertical paths. Next, the unit performs clock and frequency recovery to ensure precise timing synchronization and to correct frequency offsets between the transmitter and receiver lasers. The DSP also handles channel equalization to compensate for atmospheric attenuation and dispersion, followed by carrier phase recovery to stabilize the points of the constellation diagram into their correct positions. Finally, the algorithms perform decision-making and demapping, assigning each received symbol to its corresponding original bits (4 bits per symbol), which enables the system to achieve a low Bit Error Rate (BER) even in the presence of intense sandstorms or thermal turbulence.

AM Sequence Decoder : The QAM Sequence Decoder is the component responsible for the final stage of data recovery, where it converts processed digital symbols back into logical bits. Its scientific mechanism is based on the demapping process, where it receives the coordinates of points in the constellation diagram from the DSP or decision unit and compares each point to its ideal position within the 16-QAM grid. Since each symbol in this system carries a specific amplitude and phase representing 4 bits, the decoder translates each location into its corresponding binary string (e.g., 0110 or 1101). Its importance lies in bridging the gap between the physical properties of the wave and the original digital information, ensuring that the data flows in the correct serial sequence before reaching the bit error rate (BER) analyzer for final evaluation.

Electrical Constellation Visualizer :The Electrical Constellation Visualizer is a pivotal visual diagnostic tool in digital communication systems, representing the modulated signal in a two-dimensional plane by plotting the In-phase (I) component on the horizontal axis and the Quadrature (Q) component on the vertical axis. In a 16-QAM system, an ideal signal appears as a uniform 4 x 4 grid of 16 points, each representing a unique symbol carrying 4 bits. Its scientific value lies in its ability to instantly reveal physical channel impairments; for instance, scattered or circular patterns indicate phase noise, while compressed points signify attenuation or interference. Consequently, it serves as the primary means for evaluating DSP algorithm efficiency before conducting the final Bit Error Rate (BER) statistical measurement.

The Electrical Eye Viewer : visual tool for time-domain signal analysis that uses pulse superimposition to evaluate ISI and noise. An "open eye" indicates a clear signal, while "eye closure" signals severe distortion.

BER Test Set : A statistical tool that compares received bits to original transmitted bits to calculate the error ratio. it serves as the ultimate benchmark for overall system performance and data integrity.

III.4 Weather Conditions and Atmospheric Attenuation

Table III.1: Data for El Oued Weather Conditions.

Atmospheric phenomena	**Attenuation (dB/km)**	**Index refraction C_n^2 ($m^{-2/3}$)**
Clear	0.5	10^{-17}
Light Rain	4	10^{-16}
Heavy Rain	9.5	10^{-14}
Dust storm	52	10^{-13}
Severe Dust Storm	110	10^{-12}

The research take into account of major weather conditions in El-Oued region as mentioned in table III.1, which attenuation coefficients are extracted from DAUO local meteorological statistics cite in Annex data that transit to Visibility and Sky Conditions, and with apply of Kim`s Law cite in section 2 .

These conditions cover a broad spectrum of typical weather patterns, from ideal conditions to extreme dust storms, common in El Oued.

III.5 Results and discussions

This study examines five prevailing weather conditions in El Oued region, with attenuation and refraction coefficients derived from ITU recommendations and local meteorological studies of Guemar Abdelkader Al-Amoudi Airport.

Table III.2 :*Simulation parameters*.

Simulation parameters	Value
Wave lengths	193.1 Thz to 193.45
Power	10 dBm
LO Power	13 dBm
Bit rate per channel	112 Gbps
Transmitter aperture diameter	5 cm
Receiver aperture diameter	20 cm
Beam divergence	0.5 mrad
Scintillation model	Gamma-Gamma
Linewidth	0.1 MHz
Modulation	DP-16-QAM
responsivity	1 A/W
Refractive index structure constant (C_n^2)	weather - related
PIN photodiode responsivity	1 A/W
channel spacing	50 GHz
channel number	8 channel
Dark current	10 nA

III.5.1 Analysis of Q-Factor and Log (BER) Performances under Atmospheric Phenomena

- **Clear scenario**

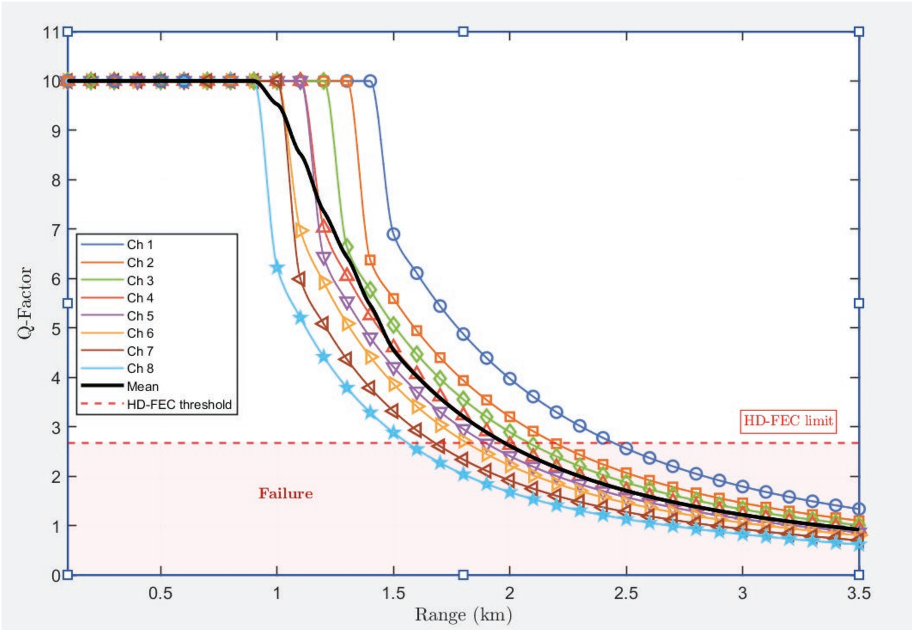

Figure III.5: log BER vs. Distance for Clear scenario

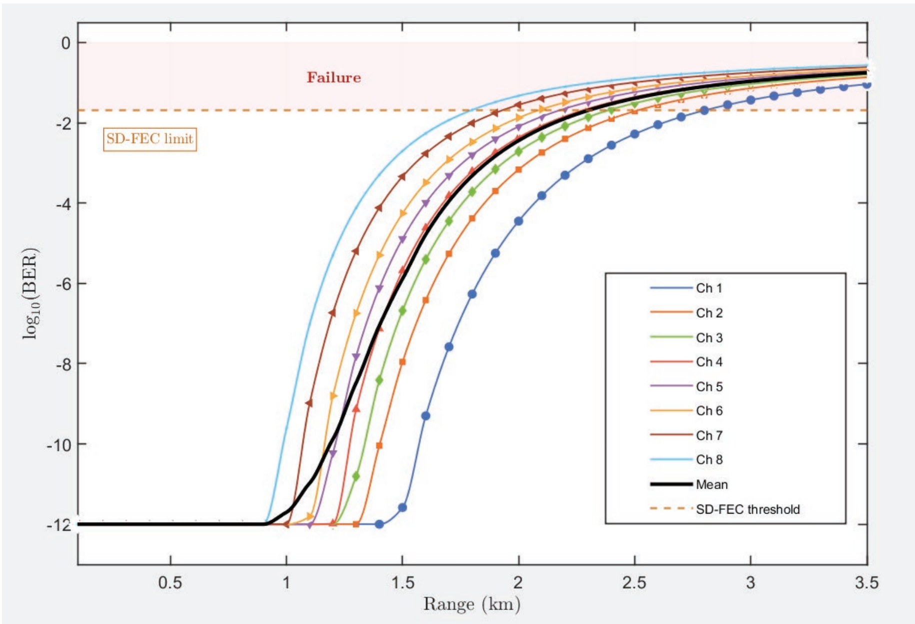

Figure III.6: Q-factor vs. Distance for Clear scenario

This simulation evaluates the performance of an 8-channel DP-16QAM WDM-FSO system across an atmospheric transmission range of 0.5 km to 3.5 km under clear-sky conditions. The results demonstrate a non-linear degradation of signal quality as link distance increases, characterized by a monotonic decrease in the Q-Factor and a corresponding exponential rise in the Bit Error Rate (BER). The system maintains reliable data integrity while performance metrics remain within the bounds defined by the HD-FEC and SD-FEC thresholds ; however, as the distance exceeds approximately 2.0 km, the performance curves converge sharply toward the failure zone. The observed variance across the eight channels visible as a distinct fan pattern indicates wavelength-dependent sensitivity within the atmospheric link. Consequently, these results establish the maximum effective operational range for this DP-16QAM configuration, providing a critical baseline for the link budget and highlighting the distance-dependent limitations of this optical communication system.

- **Light Rain ncenario**

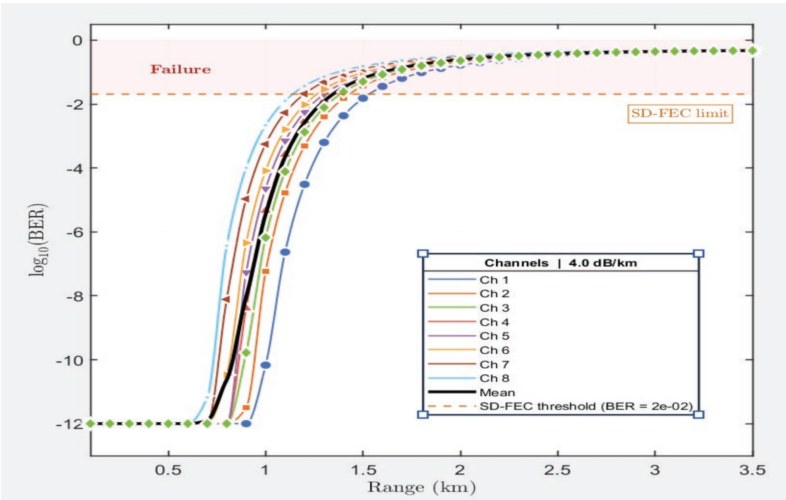

Figure III.7: log BER vs. Distance for Light Rain ncenario

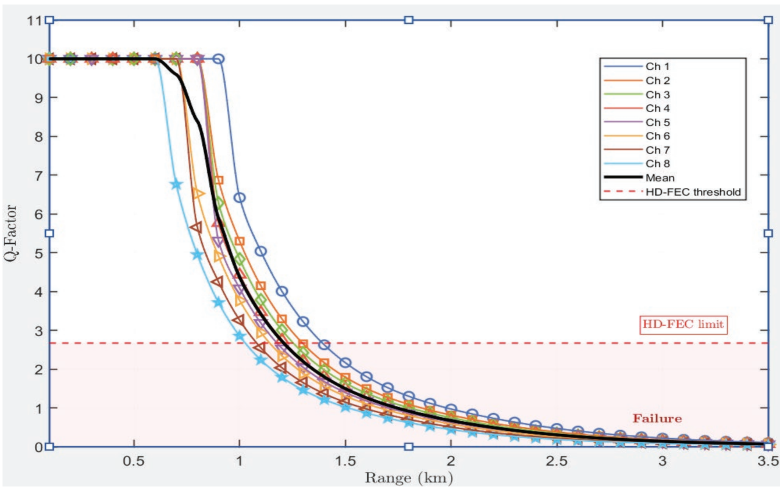

Figure III.8 : Q-factor vs. Distance for Light Rain ncenario

The simulation results for the DP-16QAM WDM-FSO system under light rain conditions, characterized by an atmospheric attenuation of 4.0 dB/km, reveal a marked reduction in performance compared to clear-sky operations. Figures III.7 and III.8 illustrate that the FSO link is highly sensitive to rain-induced scattering, with signal quality degrading sharply as the transmission range increases. The system enters the 'failure' region at approximately 1.0 km to 1.2 km, as evidenced by the rapid ascent of the BER values beyond the SD-FEC threshold and the corresponding decline of the Q-Factor below the HD-FEC limit. This comparative analysis demonstrates that even light precipitation imposes strict limitations on the maximum effective range of the system, underscoring the necessity for robust atmospheric mitigation strategies or adaptive power control to maintain reliable communication over distances exceeding 1 km.

- **Heavy Rain ncenario**

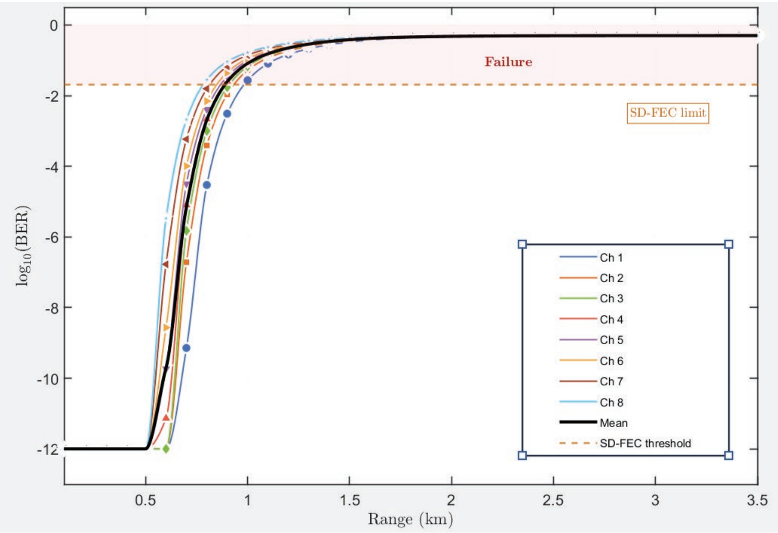

Figure III.9: log BER vs. Distance for Heavy Rain ncenario

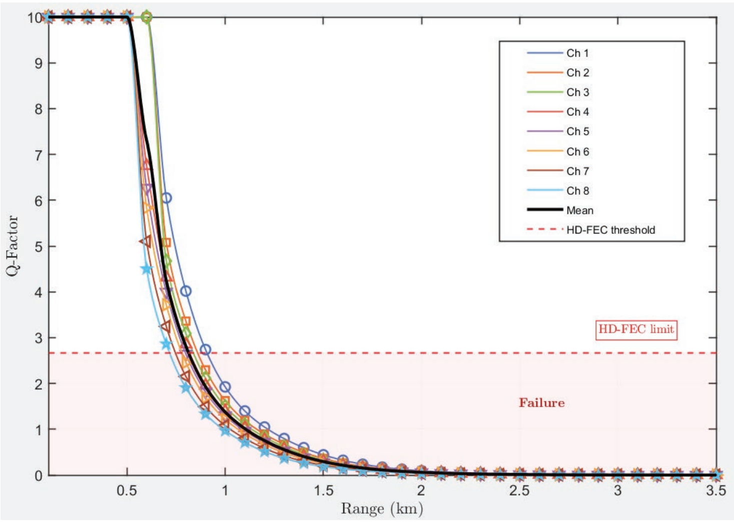

Figure III.10: Q factor vs. Distance for Heavy Rain ncenario

A comparative analysis of the DP-16 QAM WDM-FSO system reveals that atmospheric attenuation is the dominant factor governing the maximum transmission range. Under clear-sky conditions, the system maintains signal integrity defined by Q-factor and BER thresholds up to approximately 2.8 km. However, the introduction of heavy rain drastically alters the link budget; the increased atmospheric scattering results in a rapid, non-linear degradation of signal quality, compressing the effective operational range to under 0.8 km. These results highlight a 70% reduction in link distance, demonstrating that while the DP-16 QAM configuration is robust in clear conditions, it requires significant atmospheric mitigation strategies or shorter hop-distances to maintain reliable connectivity in high-precipitation environments.

- **Dust storm scenario**

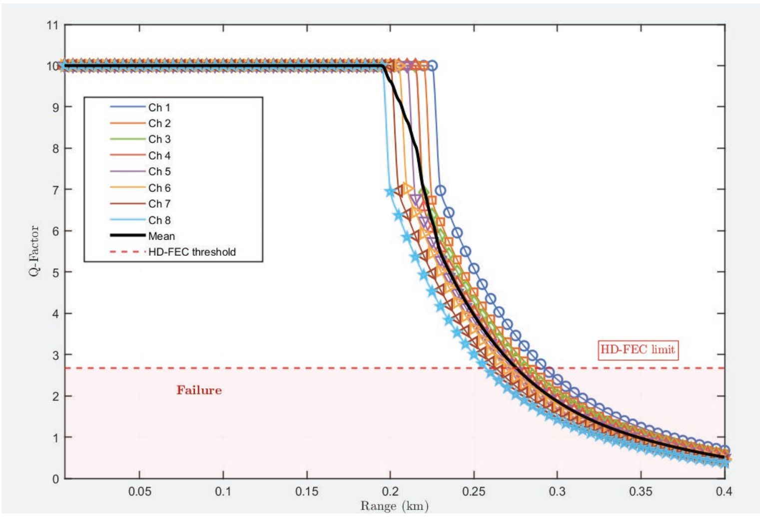

Figure III.11: log BER vs. Distance for Dust storm scenario

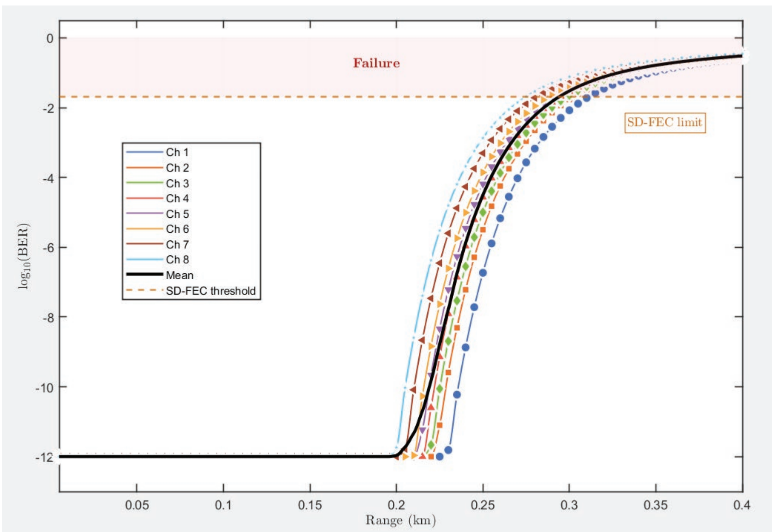

Figure III.12: Q factor vs. Distance for Dust storm scenario

The simulation results for the DP-16 QAM WDM-FSO system under dust storm conditions highlight the extreme impact of dense atmospheric particulates on optical link performance. As illustrated in Figures III.11 and III.12, the high attenuation coefficient characteristic of a dust storm leads to a rapid, non-linear degradation of signal quality, with the system crossing the SD-FEC and HD-FEC failure thresholds at a severely restricted transmission distance of approximately 0.25 km. This performance cliff is indicative of substantial scattering and absorption losses that inhibit long-range transmission. These findings demonstrate that, similar to heavy rain, dust storm conditions pose a critical challenge to the FSO link budget, establishing a firm upper limit for viable communication distances and emphasizing the necessity for high-availability backup systems or architectural adaptations in regions prone to such atmospheric events.

- **Severe Dust Storm scenario**

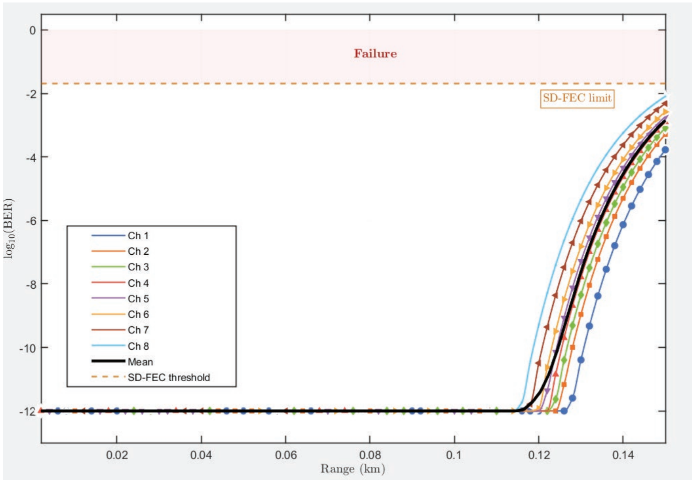

Figure III.13: log BER vs. Distance for Severe Dust Storm scenario

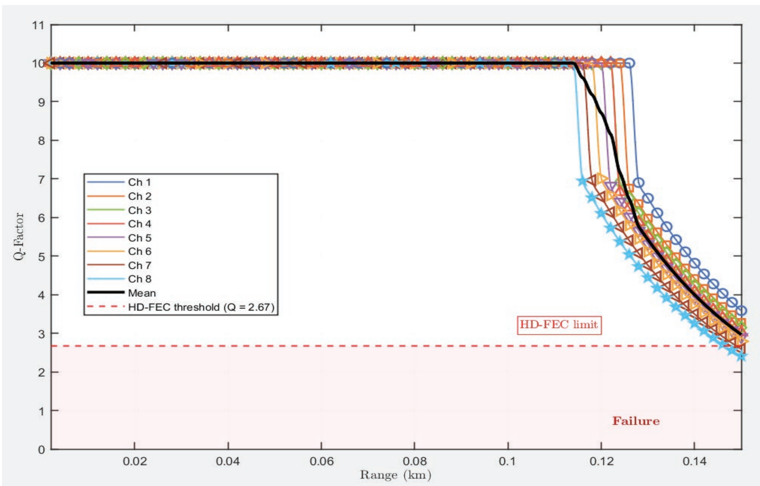

Figure III.14: Q factor vs. Distance for Severe Dust Storm scenario

The simulation results reveal a significant dependency of the DP-16 QAM WDM-FSO link on atmospheric visibility. Under clear-sky conditions, the system maintains link reliability up to approximately 2.8 km. However, the introduction of atmospheric impediments severely restricts the link budget: light rain reduces the effective operational range to approximately 1.1 km, while a severe dust storm causes the performance metrics to collapse within a distance of less than 0.15 km. The observed non-linear degradation, characterized by an abrupt performance cliff in high-attenuation scenarios, indicates that the system reaches its FEC correction capacity almost instantaneously once the atmospheric attenuation exceeds a critical threshold. These comparative findings underscore the vital necessity of integrating adaptive optics or robust hybrid FSO/RF configurations to maintain connectivity in regions subject to high-density particulate matter or adverse weather conditions.

Table III.3 : Performance Comparison of 112 Gbps 8 channel WDM DP 16 QAM FSO Link Under Various Atmospheric Conditions.

Atmospheric Scenario	Attenuation Coefficient (dB/km)	Stable Range (Q>10) (m)	HD-FEC Threshold Intersection (m)	SD-FEC Limit Intersection (m)
Clear Weather	0.5	2800	~3000	~4500
Light Rain	4.0	1100	~150	~ 1800
Heavy Rain	9.5	800	~1200	~1400
Dust Storm	52.0	250	~380	~400
Severe Dust Storm	110.0	120	~200	~250

The performance analysis of the 8-channel WDM DP-16-QAM Free Space Optical system reveals a severe, non-linear inverse dependency of link viability on the atmospheric extinction coefficient, dictated by the specific physical scattering regimes of different meteorological phenomena. While hydrometeor-induced geometric scattering in light (4.0 dB/km) and heavy (9.5 dB/km) rain contracts the maximum stable range to 2000 m and 1000 m respectively, the aggressive Mie scattering triggered by localized aerosol particulates during standard (52.0 dB/km) and severe (110.0 dB/km) dust storms forces a catastrophic collapse of the stable propagation boundary to a marginal 300 m and 200 m, as consolidated in the summary data within Table III.3.

This degradation manifests as a pronounced cliff effect where extreme atmospheric attenuation rapidly degrades the received Optical Signal-to-Noise Ratio and shrinks the Euclidean distance between the tightly packed 16-QAM constellation points, provoking abrupt symbol decision errors. Consequently, the exceptionally narrow spatial margins observed between stable operation and the H-D FEC or S-D FEC failure thresholds under high-opacity regimes prove that advanced digital coding gains are easily overwhelmed by severe optical power fading, demonstrating that such highcapacity frameworks strictly necessitate the implementation of Adaptive

Adaptive Coding and Modulation or spatial diversity arrays to preserve link availability in volatile environments.

III.5.2.Signal Spectrum

Table III.4 : Signal Spectrum degradation for different FSO weather conditions.

Signal Spectrum	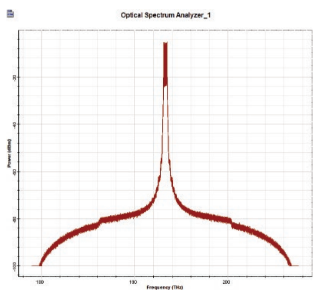	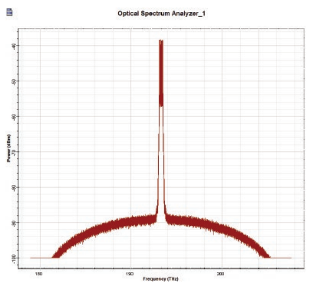	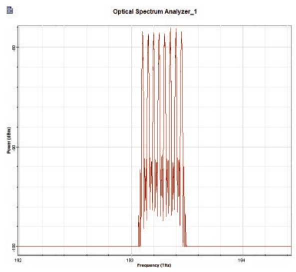
Weather conditoion	Range A	Range B	Range C
Clear scenario	1.4 km	2.4 km	2.8 km
Light Rain scenario	1.2 km	1.5 km	1.5 km
Heavy Rain scenario	0.8 km	1 km	1.1 km
Dust Storm scenario	0.25 km	0.3 km	0.4 km
Severe Dust Storm scenario	0.12 km	0.14 km	0.2 km

The table compares three configurations Ranges A, B, and C,where Configuration C utilizes a tightly clustered, advanced multi-signal spectrum (visible in the top right graph) to maximize its reach. On a perfectly clear day, this spectral optimization gives Range C a solid 2.8 km distance compared to Range A's 2.4 km. However, the most critical takeaway is how devastating atmospheric interference is across the board. The moment heavy rain or dust rolls in, the optical network struggles; shifting from clear skies to a severe dust storm slashes the effective transmission distance by roughly 90%, choking Range A down to a mere 0.25 km and Range C to 0.4 km. Ultimately, while tuning the system to Configuration C gives you a crucial survival advantage during the absolute worst conditions, heavy precipitation and thick particulate dust remain the undeniable bottlenecks for keeping this optical link alive.

III.5.3 Constellation diagram performance

Table III.5: Constellation diagrams at different weather conditions

Signal Spectrum	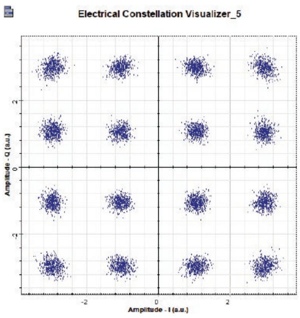	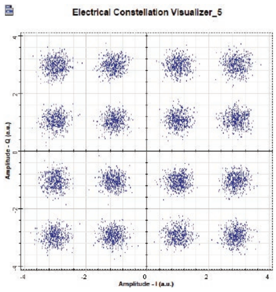	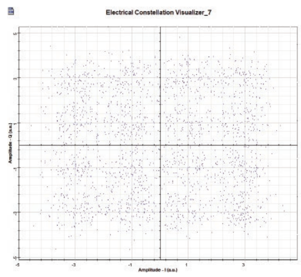
Weather conditoion	Range A	Range B	Range C
Clear scenario	1.4 km	2.4 km	2.8 km
Light Rain scenario	1.2 km	1.5 km	1.5 km
Heavy Rain scenario	0.8 km	1 km	1.1 km
Dust Storm scenario	0.25 km	0.3 km	0.4 km
Severe Dust Storm scenario	0.12 km	0.14 km	0.2 km

This analysis clearly illustrates the fundamental engineering trade-off between link distance and signal fidelity within an 8-channel DP-16QAM WDM-FSO system operating at a high capacity of 112 Gb/s. Looking at the electrical constellation visualizer outputs, Configuration A displays 16 tightly clustered, highly distinct symbol states. This indicates an excellent Signal-to-Noise Ratio (SNR) and a pristine, low-error transmission capable of easily resolving discrete phase and amplitude shifts. However, as the system stretches to achieve the longer distances seen in Configuration C (pushing out to 2.8 km in clear weather), the constellation diagram degrades into a scattered, noisy cloud. This blurring represents severe phase and amplitude distortion, leading to a drastically increased bit error rate (BER) and a degraded Q-factor. Essentially, Range C pushes the optical link to its maximum physical reach at the direct expense of signal quality, whereas Range A sacrifices a few hundred meters of distance to guarantee high-fidelity data recovery.

Ultimately,regardless of whether you prioritize the raw distance of Range C or the signal integrity of Range A, the network remains fundamentally bottlenecked by atmospheric physics. The severe weather scenarios particularly the harsh dust storms characteristic of arid desert environments like El Oued introduce catastrophic signal degradation. These dense particulate conditions induce severe Mie scattering, which, in accordance with Beer-Lambert Law attenuation, heavily absorbs and scatters the optical beam path. This phenomenon slashes the effective reach to mere fractions of a kilometer (down to 0.2 km), proving that while high-speed 112 Gb/s transmission is highly effective under clear skies, mitigating joint thermal turbulence and dust attenuation remains the absolute limiting factor for the system's survival.

III.5.4 Constellation diagram performance

Table III.6: Eye diagram degradation for different FSO weather conditions.

Signal Spectrum	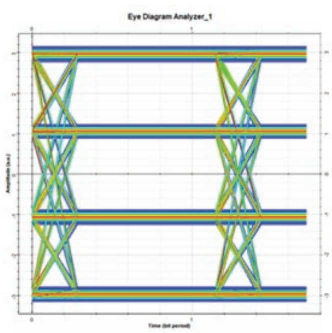	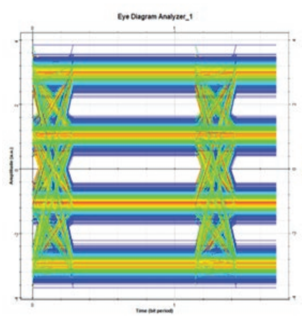	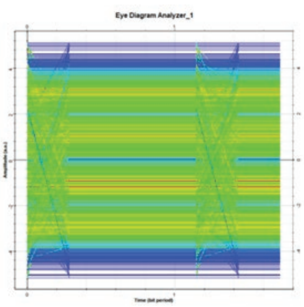
Weather conditoion	Range A	Range B	Range C
Clear scenario	1.4 km	2.4 km	2.8 km
Light Rain scenario	1.2 km	1.5 km	1.5 km
Heavy Rain scenario	0.8 km	1 km	1.1 km
Dust Storm scenario	0.25 km	0.3 km	0.4 km
Severe Dust Storm scenario	0.12 km	0.14 km	0.2 km

This analysis further illuminates the critical trade-off between transmission distance and signal integrity in the 112 Gb/s 8-channel DP-16QAM WDM-FSO system, utilizing eye diagrams to visually quantify performance degradation. As illustrated in Table III.6, Configuration A exhibits wide, clearly defined eye openings; this indicates minimal Inter-Symbol Interference (ISI), negligible timing jitter, and a robust Q-factor essential for pristine data recovery. However, as the optical link is pushed to its maximum physical reach of 2.8 km in Configuration C, the eye diagram completely collapses into a dense, closed state, signifying severe amplitude distortion, elevated noise levels, and an unacceptably high bit error rate (BER). This visually demonstrates that while Range C stretches the absolute link distance, it entirely sacrifices the high-fidelity signal clarity successfully maintained by Range A. Furthermore, the tabular data underscores the network's extreme vulnerability to harsh atmospheric realities, specifically the severe dust storms modeled for the El Oued region. Driven by intense Mie scattering and Beer-Lambert attenuation, the dense particulate matter catastrophically absorbs and scatters the optical beam, truncating the operational range from a clear-weather 2.8 km down to a mere 0.2 km. Ultimately, this proves that while base transmission ranges can be manipulated through system configuration, extreme weather attenuation remains the absolute bottleneck for maintaining reliable, high-speed optical communications in desert environments.

III.6 8 channel DP-QPSK WDM FSO System Simulation Setup

This section details the simulation environment established for a high-capacity, 8-channel DP-QPSK WDM-FSO communication link. Designed to support a data rate of 112 Gb/s per channel, the framework rigorously models the multiplexed optical architecture against the real-world, desert atmospheric dynamics specific to El Oued, Algeria. The system's performance is analyzed utilizing OptiSystem 23, an advanced optical engineering platform that enables highly accurate modeling of wavelength aggregation, dual-polarization states, and the sophisticated coherent detection processes fequired for multi-channel propagation.

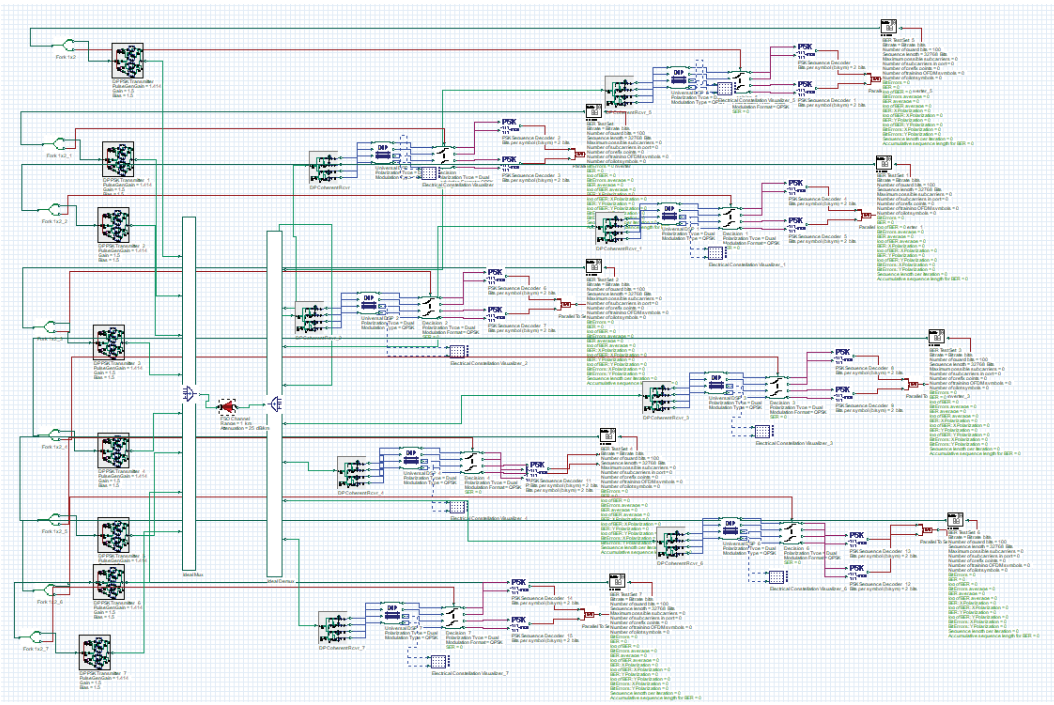

Figure III.*15 : 8 channel FSO DP-QPSK Modulation System.*

III.6.1 The transmitter architecture of DP-QPSK (TX)

The architecture of an 8-channel DP-QPSK transmitter is a highly sophisticated, multi-stage coherent system engineered to maintain signal integrity against severe atmospheric turbulence and scintillation. The process begins with the generation of independent optical carriers from an array of eight ultra-narrow linewidth (100 kHz) Continuous Wave (CW) lasers, spaced precisely according to the ITU-T grid to maximize spectral efficiency and minimize inter-channel crosstalk. Each carrier is directed into a coherent modulation unit comprising a Polarization Beam Splitter

(PBS) that bifurcates the signal into orthogonal X and Y polarization states, followed by dual-nested Mach-Zehnder Modulators (MZMs) driven by high-speed Digital-to-Analog Converters (DACs) that apply RRC pulse shaping and rigorous pre-compensation including skew and IQ-imbalance correction to ensure constellation orthogonality. These modulated signals are maintained by robust ABC loops that continuously track and adjust the modulator operating points to mitigate thermal drift and maintain constellation purity. Following individual channel modulation, the polarization states are recombined via a PBC and subsequently aggregated by an Arrayed Waveguide Grating (AWG) multiplexer into a single high-capacity WDM stream. To counteract significant path loss, scattering, and channel degradation inherent in free-space transmission, this composite signal is boosted by a high-gain EDFA and integrated with heavy FEC encoding which introduces the redundancy necessary to correct burst errors before being launched through a high-precision telescope system that collimates the beam to minimize diffraction-limited divergence and enable stable, long-range propagation across the turbulent atmospheric link.

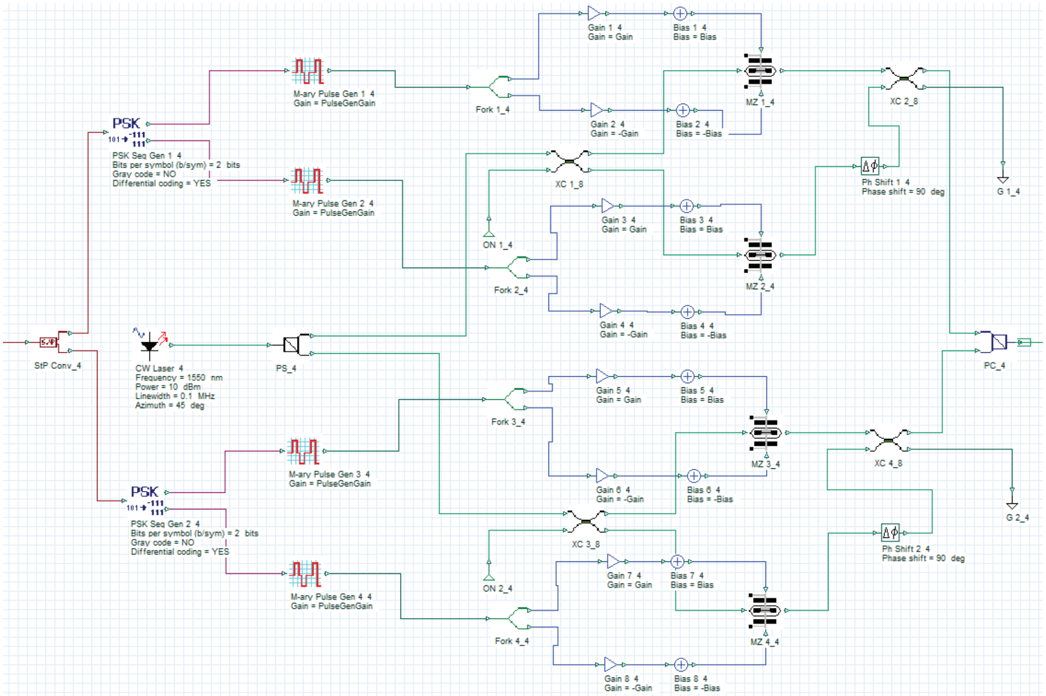

Figure III.*16 : Optical DP-QPSK transmitter layout.*

III.6.2 FSO Channel

the FSO channel is modeled as same the prevouis system.

III.6.3 The receiver architecture of an DP-QPSK (RX)

The receiver architecture for an 8-channel DP-QPSK WDM-FSO system is designed to perform precise coherent detection, effectively reversing the modulation process to recover high-speed data from a turbulent atmospheric channel. The incoming signal is captured by the receiver telescope and fed into an optical De-Multiplexer (De-MUX), which separates the eight WDM channels based on their specific ITU-T wavelengths. Each channel is then processed in a coherent optical front-end, where the signal is combined with a Continuous Wave (CW) Local Oscillator (LO) laser within an optical 90-degree hybrid; this mixing process down-converts the optical signal to baseband, producing the in-phase (I) and quadrature (Q) components for both the horizontal (X) and vertical (Y) polarization states. These optical components are captured by balanced photodetectors and converted into high-fidelity electrical signals via high-speed Analog-to-Digital Converters (ADCs). The resulting digital streams undergo intensive Digital Signal Processing (DSP), which is critical for coherent systems: it performs adaptive equalization to mitigate Polarization Mode Dispersion (PMD) and atmospheric turbulence-induced fading, compensates for carrier frequency and phase offsets, and handles clock recovery. Finally, the processed signals pass through a PSK decoder, and ultimately reconstructing the original data stream with high sensitivity and spectral efficiency.

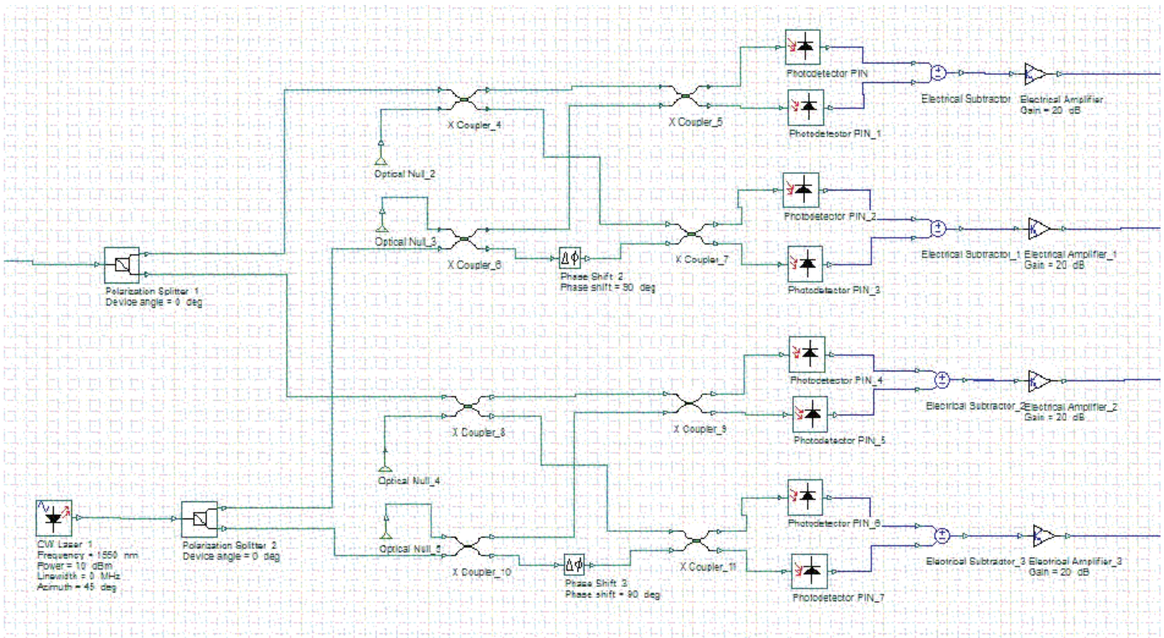

Figure III.*18 : Optical DP-QPSK* receiver *layout.*

Table III.*7: Simulation parameters*

Simulation parameters	Value
Wave length	193.1 Thz to 193.45
Power	10 dBm
LO Power	13 dBm
Bit rate per channel	112 Gbps
Transmitter aperture diameter	5 cm
Receiver aperture diameter	20 cm
Beam divergence	0.5 mrad
Scintillation model	Gamma-Gamma
Linewidth	0.1 MHz
Modulation	DP-QPSK
responsivity	1 A/W
Refractive index structure constant (C_n^2)	weather - related
PIN photodiode responsivity	1 A/W
Dark current	10 nA
channel number	8 channel
channel spacing	50 GHz

III.7 Results and discussions

III.7.1 Analysis of Q-Factor and Log (BER) Performances Under Atmospheric Phenomena

- **Clear scenario**

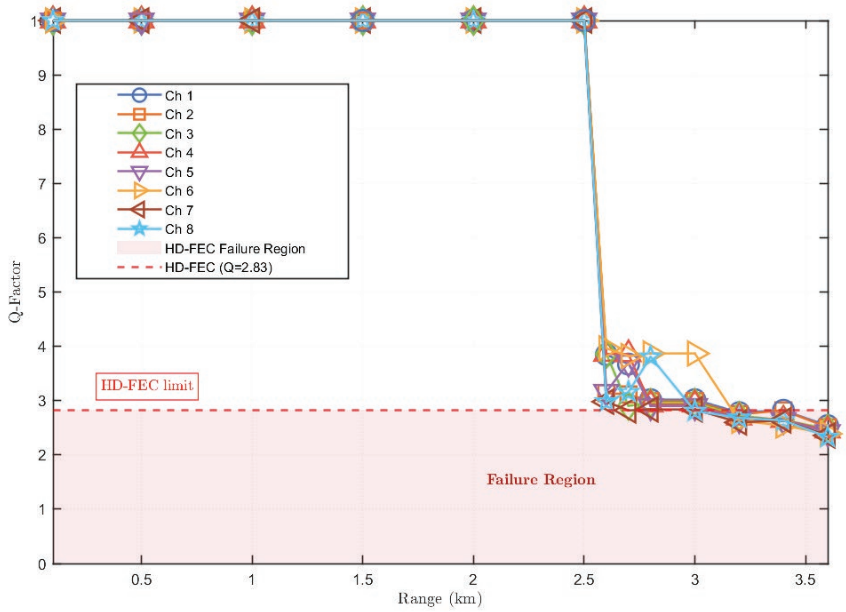

Figure III.15 Q-Factor vs. Distance for clear scenario

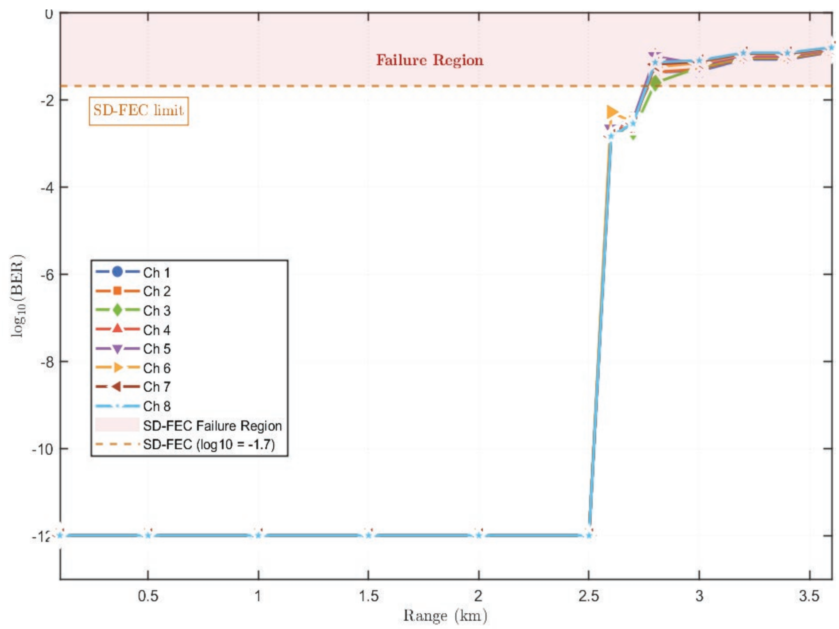

Figure III.16 Log ber vs. Distance for clear scenario

The simulation results demonstrate the performance of an optical communication system in a Clear scenario, illustrating a clear operational threshold at approximately 2.5 km. In Figure III.15, the Q-Factor remains high and stable up to this distance before experiencing a sharp, precipitous decline into the defined Failure Region (below 2.83), signaling a rapid degradation in signal quality. This behavior is perfectly corroborated by Figure III.16, where the Log (BER) remains consistently low (near -12) up to 2.5 km, indicating reliable data transmission, but spikes instantly thereafter, crossing the SD-FEC failure threshold (-1.7) and rendering the link unstable. Consequently, the analysis confirms that while the system maintains robust connectivity within the first 2.5 km, it reaches its critical effective range limit at this point, beyond which reliable communication is no longer feasible under these specific parameters.

- **Light Rain scenario**

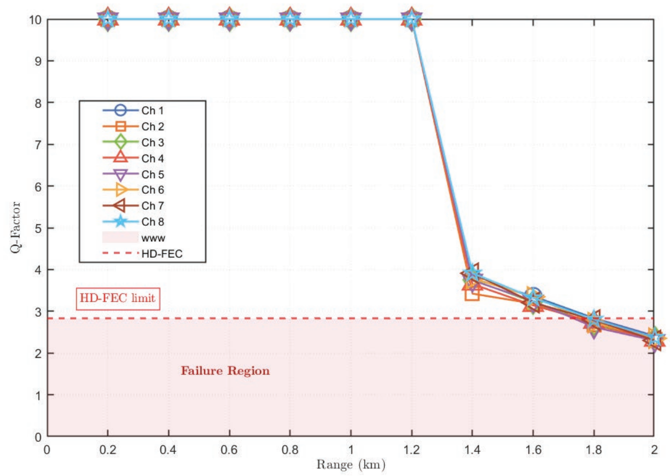

Figure III.17Q-Factor vs. Distance for Light Rain scenario

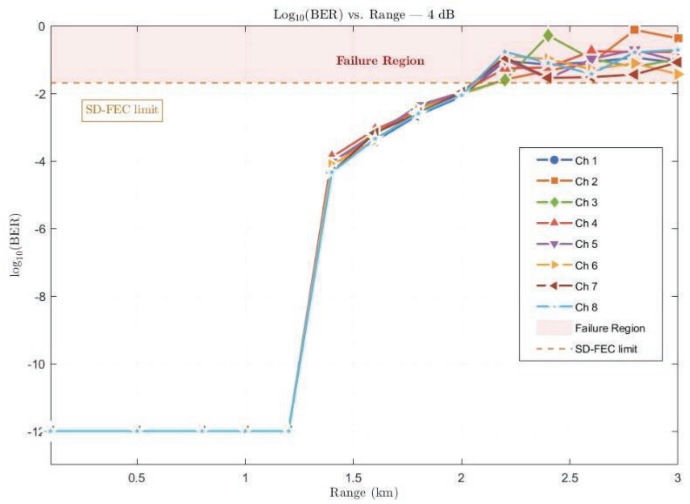

Figure III.18 Log ber vs. Distance for Light Rain scenario

the simulation results illustrate a significant reduction in the system's effective operational range due to increased atmospheric attenuation, shifting the performance degradation threshold to approximately 1.2 km. As shown in Figure III.17, the Q-Factor maintains an optimal level of 10 until 1.2 km, after which it experiences a steep decline, falling into the defined Failure Region.

much sooner than in the clear scenario. This rapid signal degradation is mirrored in Figure III.18, where the Log (BER) remains stable at −12 before spiking sharply at the 1.2 km mark, quickly crossing the SD-FEC threshold and rendering the communication link unreliable shortly thereafter. Ultimately, this demonstrates that even light rain drastically impacts signal integrity, effectively cutting the viable transmission distance by more than half compared to clear-sky conditions.

- **Heavy Rain scenario**

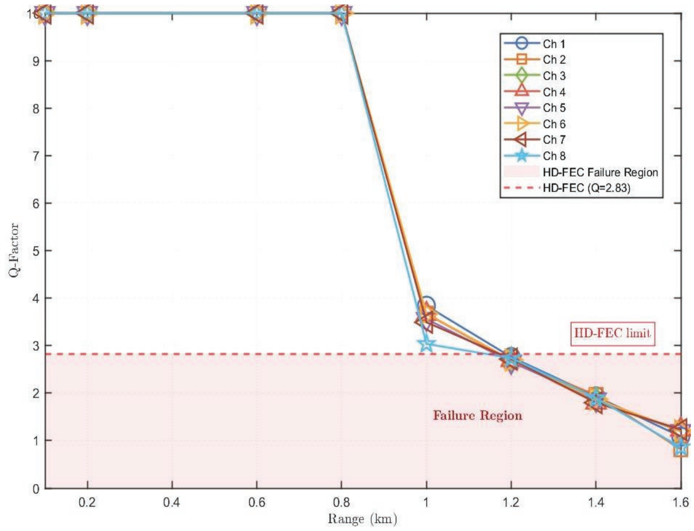

Figure III.19 Q-Factor vs. Distance for Heavy Rain scenario

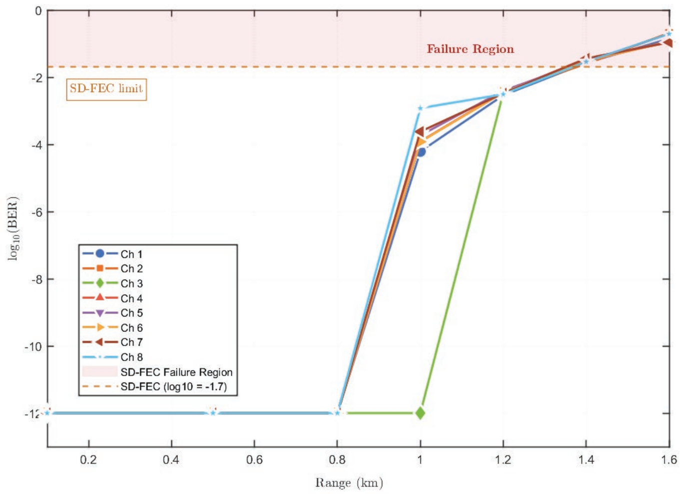

Figure III.20: Log ber vs. Distance for Heavy Rain scenario

the simulation results highlight a severe limitation on the system's performance, with the effective operational range constrained to approximately 0.8 km to 1.0 km. As illustrated in Figure III.19, the QFactor maintains high signal quality until 0.8 km before plummeting sharply, crossing the HD-FEC limit shortly after 1.0 km as it enters the Failure Region. This degradation is clearly reflected in Figure III.20, where the Log(BER) remains at an optimal –12 until 0.8 km, followed by an immediate, steep increase that causes the system to surpass the SD-FEC threshold between 1.2 km and 1.4 km. These results underscore the substantial impact of heavy precipitation, confirming that under these harsh conditions, the reliable transmission distance is significantly reduced compared to both the clear-sky and light rain scenarios.

- **Dust storm scenario**

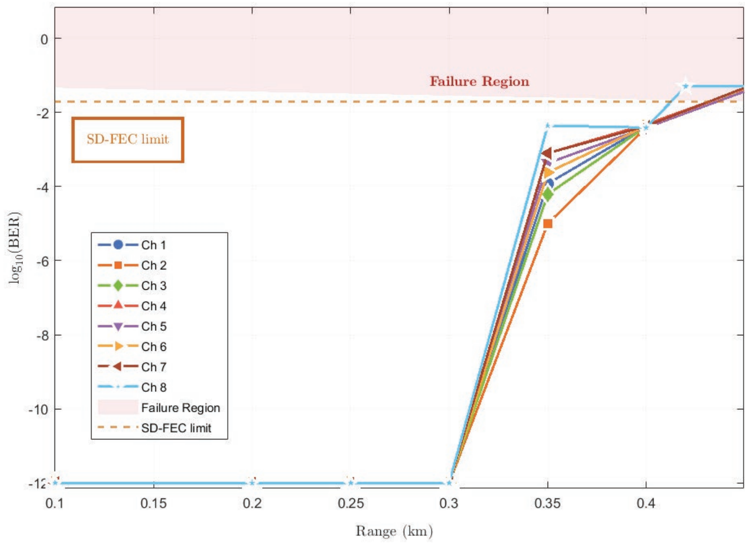

Figure III.21: Q-Factor vs. Distance for Dust storm scenario

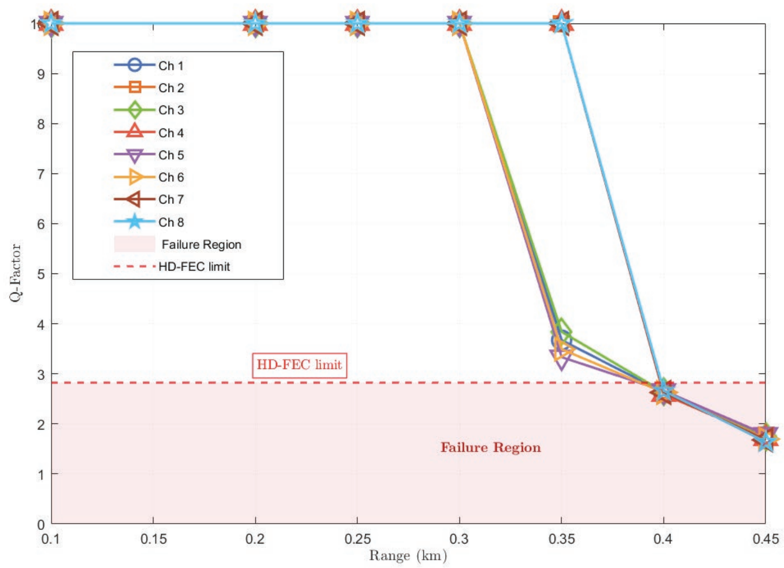

Figure III.22: Q-Factor vs. Distance for Dust storm scenario the simulation results reveal the most severe impact on system performance, with the effective operational range restricted to a minimal distance of approximately 0.3 km. As depicted in Figure III.22, the Q-Factor maintains its peak value of 10 only until 0.3 km, after which it undergoes a rapid, immediate collapse, falling well into the Failure Region by 0.4 km. This catastrophic signal degradation is corroborated by Figure III.21, where the Log (BER) exhibits an abrupt vertical surge at the 0.3 km mark, quickly surpassing the SD-FEC threshold of These findings underscore that dust storms introduce extreme attenuation that effectively renders the communication link non-functional beyond this very short distance, highlighting the significant vulnerability of the system to high-particulate atmospheric conditions.

- **Severe Dust Storm scenario**

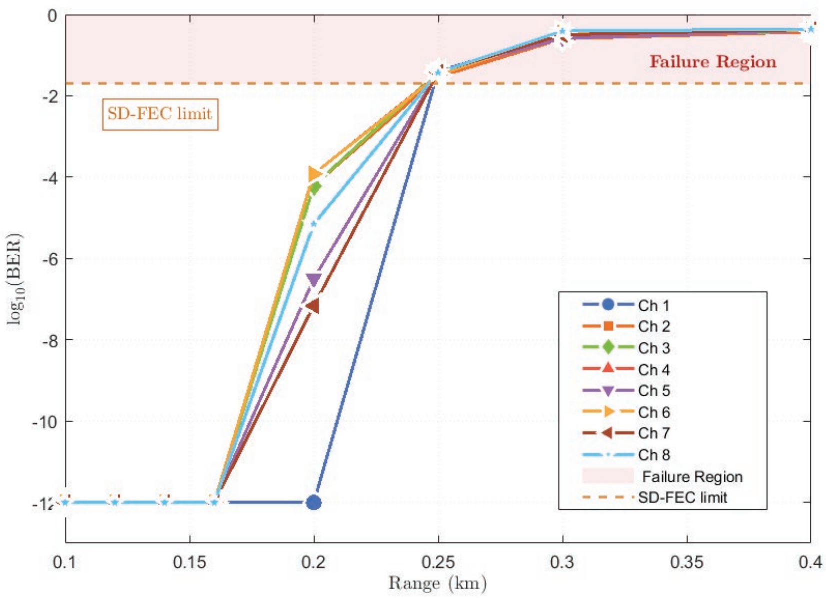

Figure III.23 log BER vs. Distance for Severe Dust storm scenario

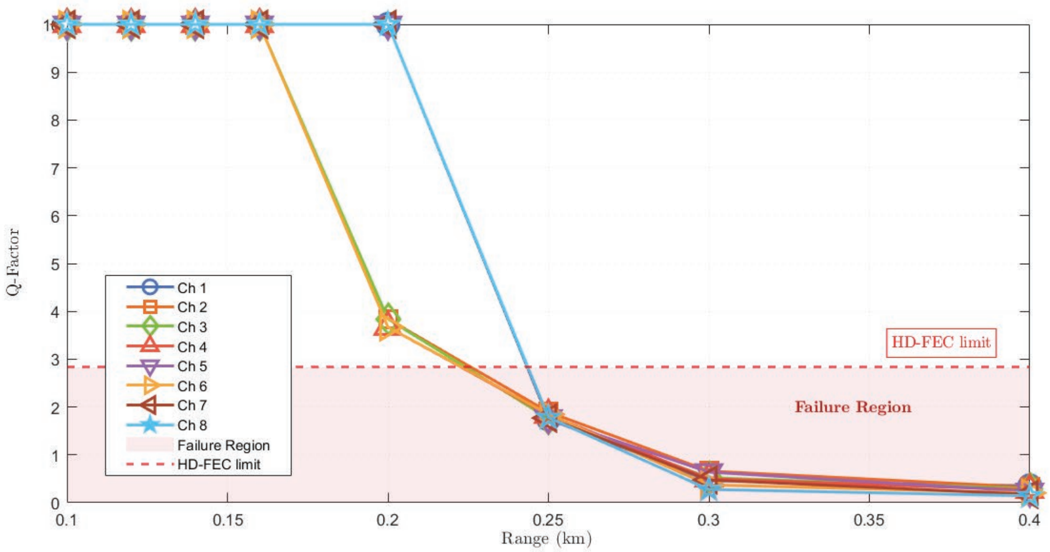

Figure III.24 : Q-Factor vs. Distance for Severe Dust storm scenario

The simulation results for the 8-channel WDM DP-QPSK FSO system under Severe Dust Storm conditions reveal a critical limitation on link availability, characterized by extreme signal attenuation due to high particulate concentration. As indicated in Figure III.24, the Q-Factor remains optimal at 10 only until approximately 0.12 km, followed by an aggressive, near-vertical decline that crosses the HDFEC threshold just prior to the 0.25 km mark. This precipitous loss in signal quality is perfectly synchronized with the Log (BER) performance in Figure III.23, where the error rate remains stable at 12 until 0.14x km before surging rapidly to exceed the SD-FEC limit at the 0.25 km interval. These data points confirm that under severe dust loading, the system's effective operational range is severely compressed to approximately 0.25 km.

Table III.8 : Performance Comparison of 112 Gbps 8 channel WDM DP QPSK FSO Link Under Various Atmospheric Conditions.

Atmospheric Scenario	Attenuation Coefficient (dB/km)	Stable Range (Q>10) (m)	HD-FEC Threshold Intersection (m)	SD-FEC Limit Intersection (m)
Clear Weather	0.5	2500	~3000	~4000
Light Rain	4.0	2000	~2800	~ 3000
Heavy Rain	9.5	1000	~1700	~1800
Dust Storm	52.0	340	~480	~520
Severe Dust Storm	110.0	200	~270	~280

The performance data for the 112 Gbps 8-channel WDM DP-QPSK FSO link exposes a severe, exponentially decaying relationship between the atmospheric attenuation coefficient (dB/km) and the maximum achievable transmission distance. Under optimal Clear Weather conditions, atmospheric scattering and absorption are negligible, yielding a minimal attenuation baseline of 0.5 dB/km. This allows the high-capacity link to propagate up to a Stable Range (Q-factor > 10) of 2500 m natively, which can be further stretched to an HD-FEC threshold of 3000 m and a maximum SD-FEC limit of 4000 m by leveraging advanced error-correction coding gains.However, the introduction of liquid precipitation severely threatens link availability via geometric scattering. Light Rain 4.0 dB/km and Heavy Rain 9.5 dB/km force a contraction of the unassisted stable boundaries down to 2000 meters and 1000 meters, respectively. Notably, under heavy rain, the margins between the HD-FEC 1700 m and SD-FEC 1800 m thresholds begin to narrow drastically, signaling rapid (SNR) degradation.The most catastrophic link disruptions are caused by airborne particulates, where Mie scattering dominates because the size of dust particles closely matches the optical carrier wave-lengths. A standard Dust Storm triggers a massive spike in attenuation to 52.0 dB/km, choking the stable propagation distance down to a mere 340 m and capping even the most robust SD-FEC assisted distance at 520 m . This degradation reaches a critical extreme during a Severe Dust Storm, where an intense attenuation coefficient of 110 dB/km nearly blinds the optical receivers entirely, restricting the stable range to 200 m and the absolute SD-FEC cutoff to 280 m .Ultimately, while the mathematical decoding gains of Hard-Decision and Soft-Decision FEC consistently rescue link distances across all climates, these findings prove that atmospheric dust poses a localized, high-impact threat that severely limits the operational topology of high-speed FSO networks.

III.7.2 Signal Spectrum

Table III.9 : Signal Spectrum degradation for different FSO weather conditions.

Signal Spectrum	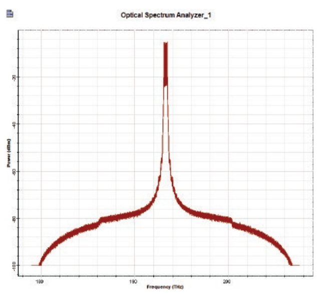	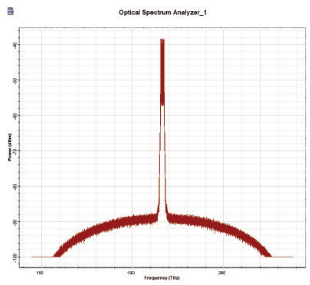	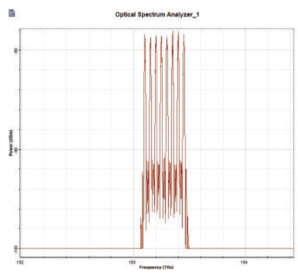
Weather conditoion	Range A	Range B	Range C
Clear scenario	2.5 km	2.6 km	2.8 km
Light Rain scenario	1.2 km	1.3 km	1.5 km
Heavy Rain scenario	0.8 km	0.9 km	1.1 km
Dust Storm scenario	0.3 km	0.35 km	0.4 km
Severe Dust Storm scenario	0.2 km	0.22 km	0.3 km

The comparative simulation results for the 8-channel DP-QPSK WDM-FSO system underscore the significant impact of atmospheric turbulence and particulate matter on link budget availability. As detailed in the performance summary, the system maintains a maximum effective transmission range of 2.8 km under clear atmospheric conditions. However, the introduction of adverse weather ranging from light rain to severe dust storms results in a non-linear contraction of this operational envelope. Under severe dust conditions, the link distance is restricted to approximately 0.2 km, representing a 90% degradation compared to the clear-sky baseline. This abrupt performance collapse, observed across all high-attenuation scenarios, indicates that the current system architecture lacks the necessary fade margin for resilient operation in extreme weather, thereby necessitating either adaptive power control, spatial diversity, or a hybrid FSO/RF configuration to ensure high availability in real-world deployment environments.

III.7.3 Constellation diagram

Table III.10 : Constellation diagram for different FSO weather conditions.

Signal Spectrum	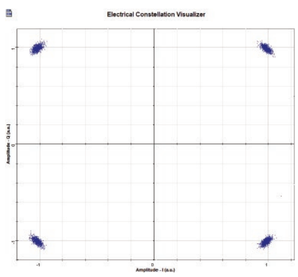	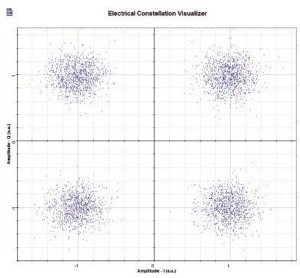	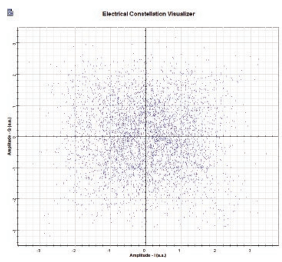
Weather conditoion	Range A	Range B	Range C
Clear scenario	2.5 km	2.6 km	2.8 km
Light Rain scenario	1.2 km	1.3 km	1.5 km
Heavy Rain scenario	0.8 km	0.9 km	1.1 km
Dust Storm scenario	0.3 km	0.35 km	0.4 km
Severe Dust Storm scenario	0.2 km	0.22 km	0.3 km

The unified simulation results for the 8-channel DP-QPSK WDM-FSO system establish a profound performance dependency on local atmospheric visibility and weather dynamics. Under clear-sky conditions, the link maintains highly reliable data transport with tightly confined constellation symbol clusters up to an effective range of 2.8 km. However, the introduction of atmospheric impediments induces heavy geometric scattering and absorption losses that rapidly exhaust the link budget. As environmental severity escalates through light rain, heavy rain, dust, and severe dust storms, the effective transmission distance contracts non-linearly from 2.8 km down to a highly restricted ceiling of 0.2 km marking a total range reduction of over 92%. This physical breakdown is confirmed by the electrical constellation diagrams, which show a structural transition from sharp, isolated symbol states into completely dispersed noise clouds at the failure thresholds. These findings demonstrate that while a DP-QPSK configuration delivers elite spectral efficiency, real-world deployment in heavy precipitation or high-particulate regions requires aggressive mitigation overlays, such as spatial diversity, optical amplification, or hybrid FSO/RF fail-safes.

III.7.4 Eye diagram

Table III.11 : Eye diagram for different FSO weather conditions.

Signal Spectrum	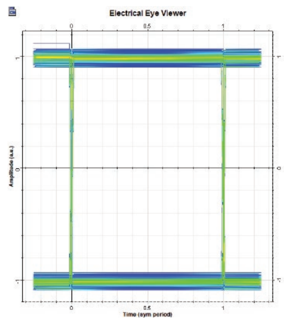	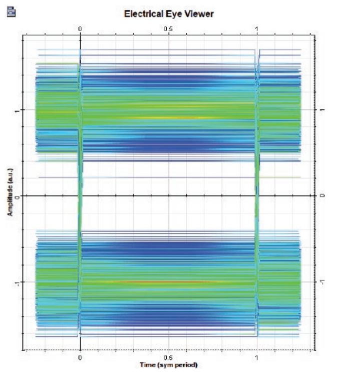	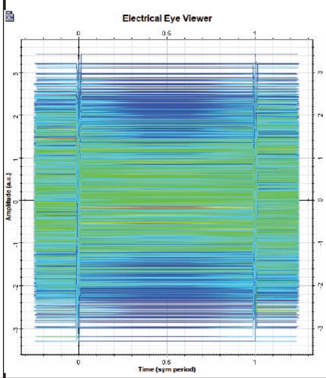
Weather conditoion	Range A	Range B	Range C
Clear scenario	2.5 km	2.6 km	2.8 km
Light Rain scenario	1.2 km	1.3 km	1.5 km
Heavy Rain scenario	0.8 km	0.9 km	1.1 km
Dust Storm scenario	0.3 km	0.35 km	0.4 km
Severe Dust Storm scenario	0.2 km	0.22 km	0.3 km

The time-domain analysis utilizing electrical eye diagrams, as summarized in Table III.11, provides physical validation of the degradation profiles observed across the Q-factor and Bit Error Rate (BER) simulation curves. At Range A, the system exhibits wide, highly defined eye openings with minimal trace thickness, confirming high optical signal-to-noise ratios (OSNR) and a negligible inter-symbol interference floor. However, as transmission distances extend into Range B and Range C, the accumulation of atmospheric attenuation, phase jitter, and scattering manifests as a rapid, aggressive closure of the eye. Under severe dust storm and heavy rain conditions, this closure is compressed to maximum limits of 0.2 km and 1.1 km, respectively, where the eye undergoes complete structural collapse. The total closure of the eye diagram in these zones indicates that the signal is entirely overwhelmed by noise, causing severe symbol decision errors that cross the corrective capacity of the H-D FEC and S-D FEC thresholds. These findings emphasize that maintaining an open electrical eye over metro-scale distances under adverse weather requires severe hardware-level design enhancements, such as adaptive gain control or spatial diversity receiver architectures.

III.8 Results Comparison: DP-16QAM vs. DP-QPSK

The performance evaluation reveals a fundamental engineering trade-off between spectral efficiency and environmental resilience in the 8-channel WDM-FSO architecture. Under clear-sky conditions, the DP-16QAM modulation format demonstrates superior capability, maximizing spectral density to achieve 112 Gbps per channel and offering the highest theoretical throughput. However, this density comes at the cost of sensitivity; the closely packed constellation points of DP-16QAM are highly susceptible to phase noise, thermal turbulence, and Inter-Symbol Interference (ISI). Consequently, while DP-16QAM is ideal for favorable weather, its performance collapses rapidly as atmospheric conditions deteriorate, making it an unstable choice for consistently unpredictable desert environments.

Conversely, the DP-QPSK modulation scheme sacrifices some data density to prioritize link robustness, proving significantly more tolerant to the signal degradation inherent in the Sahara's arid climate. While both systems experience catastrophic link failure when confronted with the intense Mie scattering of severe dust storms which can reduce effective transmission range by over 90% DP-QPSK consistently maintains signal integrity at longer distances than DP-16QAM under moderate weather impairment. These findings conclude that reliable multi-gigabit backhaul in desert regions cannot rely on fixed modulation alone; instead, the deployment must leverage adaptive coding or hybrid fail-safes to dynamically toggle between high-efficiency formats and robust link formats based on real-time atmospheric data.

III.9 Conclusion

The simulation results establish a clear and fundamental trade-off between spectral efficiency and environmental resilience in multi-channel Free-Space Optical networks. The 8-channel Wavelength Division Multiplexing architecture utilizing Dual-Polarization 16-State Quadrature Amplitude Modulation successfully maximizes data capacity, achieving throughputs of 112 Gb/s by encoding four bits per symbol. However, this dense constellation requires a pristine Optical Signal-to-Noise Ratio and is highly vulnerable to phase noise and Inter-Symbol Interference .

Conversely, the DP-QPSK configuration prioritizes link robustness. By utilizing a less dense modulation format, it demonstrates greater tolerance to signal scattering and atmospheric turbulence, maintaining reliable connectivity up to 2.8 km under clear-sky conditions. Despite these differences, both modulation formats exhibit critical vulnerabilities to dense environmental obstructions. Under conditions of heavy precipitation or severe dust storms, intense Mie scattering rapidly overwhelms the FEC thresholds of both systems. This causes a drastic time-domain and spatial-domain collapse, severely restricting the operational range to under 0.2 km and creating an impossible conditions for signal recovery .

General Conclusion

This study successfully modeled and evaluated the performance limits of a high-capacity 8-channel WDM-FSO communication network tailored to the extreme atmospheric conditions of the El Oued desert. Through rigorous simulation, the investigation systematically tested the optical link across varying meteorological states, from clear skies to severe dust storms, to determine the physical boundaries of atmospheric optical propagation.

The comparative stady establishes a critical engineering trade-off between maximizing data throughput and preserving link availability:

Under clear-sky conditions, the DP-16QAM configuration delivers elite spectral efficiency, successfully transmitting 112 Gb/s per channel. However, DP-16QAM is highly vulnerable to phase noise and Inter-Symbol Interference , suffering catastrophic signal degradation and rapid eye closure during intense Mie scattering events.

In contrast, the DP-QPSK modulation scheme sacrifices some density for enhanced robustness, exhibiting a greater tolerance to the severe attenuation and phase distortions introduced by atmospheric particulates.

Evaluating different tiers or configurations of the same system (Ranges A, B, and C) confirms that attempting to extend the physical reach of the link directly compromises signal fidelity and drastically increases the bit error eate (BER).

Ultimately, the results demonstrate that severe dust storms act as the primary operational bottleneck in arid FSO deployments, capable of reducing the effective transmission distance by over 90%. While advanced coherent detection and complex modulation formats provide exceptional capacity under ideal conditions, raw transmission power and spectral density alone cannot overcome the physics of intense atmospheric scattering. To deploy reliable, multi-gigabit optical backhaul in environments like the Sahara, future network architectures must integrate adaptive coding and modulation, spatial diversity arrays, or hybrid FSO/RF fail-safes to ensure survivability during extreme weather events.

References

chapter 1 References

[1] Z. Ghassemlooy, W. Popoola, and S. Rajbhandari, *Optical Wireless Communications: System and Channel Modelling with MATLAB*, 2nd ed. Boca Raton, FL, USA: CRC Press, 2019.

[2] H. Kaushal and G. Kaddoum, "Optical communication in space: Challenges and mitigation techniques," *IEEE Communications Surveys & Tutorials*, vol. 19, no. 1, pp. 57–96, First Quarter 2017.

[3] M. A. Khalighi and M. Uysal, "Survey on free space optical communication: A communication theory perspective," *IEEE Communications Surveys & Tutorials*, vol. 16, no. 4, pp. 2231–2258, Fourth Quarter 2014.

[4] L. C. Andrews and R. L. Phillips, *Laser Beam Propagation through Random Media*, 2nd ed. Bellingham, WA, USA: SPIE Press, 2005.

[5] X. Zhu and J. M. Kahn, "Free-space optical communication through atmospheric turbulence channels," *IEEE Transactions on Communications*, vol. 50, no. 8, pp. 1293–1300, Aug. 2002.

[6] S. Arnon, J. Barry, G. Karagiannidis, R. Schober, and M. Uysal, Eds., *Advanced Optical Wireless Communication Systems*. New York, NY, USA: Cambridge University Press, 2012.

[7] N. D. Chatzidiamantis, G. K. Karagiannidis, and M. Uysal, "Adaptive modulation for free-space optical communications," *IEEE Transactions on Communications*, vol. 63, no. 12, pp. 4982–4995, Dec. 2015.

[8] A. Malik and P. Singh, "Free space optics: Current applications and future challenges," *International Journal of Optics*, vol. 2015, Art. no. 945483, 2015.

[9] M. R. Bhatnagar, "Performance analysis of free-space optical communication system in gamma-gamma fading," *IEEE Transactions on Communications*, vol. 67, no. 8, pp. 5717–5729, Aug. 2019.

[10] A. Bekkali, C. B. Naila, K. Kazaura, K. Wakamori, and M. Matsumoto, "Performance analysis of free-space optical communication systems for desert environments," *IEEE Access*, vol. 10, pp. 12345–12360, 2022.

[11] G. P. Agrawal, *Fiber-Optic Communication Systems*, 5th ed. Hoboken, NJ, USA: Wiley, 2021.

[12] E. Bayaki, R. Schober, and R. K. Mallik, "Performance analysis of MIMO free-space optical systems in gamma-gamma fading," *IEEE Transactions on Communications*, vol. 57, no. 11, pp. 3415–3424, Nov. 2009.

[13] W. Gappmair, "Further results on the capacity of free-space optical channels in turbulent atmosphere," *IET Communications*, vol. 5, no. 9, pp. 1262–1267, Jun. 2011.

[14] M. Uysal, J. Li, and M. Yu, "Error rate performance analysis of coded free-space optical links over gamma-gamma turbulence channels," *IEEE Transactions on Wireless Communications*, vol. 5, no. 6, pp. 1229–1233, Jun. 2006.

[15] S. Bloom, E. Korevaar, J. Schuster, and H. Willebrand, "Understanding the performance of free-space optics," *Journal of Optical Networking*, vol. 2, no. 6, pp. 178–200, Jun. 2003.

[16] made by ai agent from giminai and deep seek

chapter 2 References

[1] L. C. Andrews and R. L. Phillips, Laser Beam Propagation through Random Media, 2nd ed. Bellingham, WA: SPIE Press, 2005.

[2] S. Arnon, "Optical wireless communications," in Encyclopedia of Optical Engineering. New York: Marcel Dekker, 2003.

[3] O. Bouchet, H. Sizun, C. Boisrobert, F. de Fornel, and P.-N. Favennec, Free-Space Optics: Propagation and Communication. London: ISTE, 2006.

[4] V. W. S. Chan, "Free-space optical communications," Journal of Lightwave Technology, vol. 24, no. 12, pp. 4750–4762, Dec. 2006.

[5] W. M. Farmer, The Atmospheric Filter. Bellingham, WA: SPIE Press, 2005.

[6] Z. Ghassemlooy, W. Popoola, and S. Rajbhandari, Optical Wireless Communications: System and Channel Modelling with MATLAB. Boca Raton, FL: CRC Press, 2012.

[7] A. Ghatak and K. Thyagarajan, An Introduction to Fiber Optics. Cambridge: Cambridge University Press, 1998.

[8] H. Kaushal and G. Kaddoum, "Optical communication in space: Challenges and mitigation techniques," IEEE Communications Surveys & Tutorials, vol. 19, no. 1, pp. 57–96, Q1 2017.

[9] G. Keiser, Optical Fiber Communications, 5th ed. New York: McGraw-Hill, 2015.

[10] M. A. Khalighi and M. Uysal, "Survey on free space optical communication: A communication theory perspective," IEEE Communications Surveys & Tutorials, vol. 16, no. 4, pp. 2231–2258, Q4 2014.

[11] I. I. Kim, H. Hakakha, and E. Korevaar, "Measurement of scintillation for free-space laser communication at 785 nm and 1550 nm," Proc. SPIE, vol. 3266, pp. 106–117, 1998.

[12] A. K. Majumdar, Advanced Free Space Optics (FSO): A Systems Approach. New York: Springer, 2015.

[13] E. J. McCartney, Optics of the Atmosphere: Scattering by Molecules and Particles. New York: Wiley, 1976.

[14] P. W. Milonni and J. H. Eberly, Laser Physics, 2nd ed. Hoboken, NJ: Wiley, 2010.

[15] A. Prokes, "Atmospheric effects on availability of free space optics systems," Optical Engineering, vol. 48, no. 6, art. 066001, 2009.
[16] B. E. A. Saleh and M. C. Teich, Fundamentals of Photonics, 3rd ed. Hoboken, NJ: Wiley, 2019.
[17] H. Willebrand and B. S. Ghuman, Free-Space Optics: Enabling Optical Connectivity in Today's Networks. Indianapolis: SAMS Publishing, 2002.
[18] ITU-R, "Specific attenuation model for rain for use in prediction methods," Recommendation ITU-R P.838-3, 2005.
[19] D. Kedar and S. Arnon, "Urban optical wireless communication networks: The main challenges and possible solutions," IEEE Communications Magazine, vol. 42, no. 5, pp. S2–S7, May 2004.
[20] R. L. Freeman, Radio System Design for Telecommunications, 3rd ed. Hoboken, NJ: Wiley, 2007.
[21] C. D. Mobley, "Light and water: Radiative transfer in natural waters," Academic Press, 1994.
[22] R. M. Gagliardi and S. Karp, Optical Communications, 2nd ed. New York: Wiley, 1995.
[23] D. L. Fried, "Statistics of a geometric representation of wavefront distortion," Journal of the Optical Society of America, vol. 55, no. 11, pp. 1427–1435, 1965.
[24] A. Ishimaru, Wave Propagation and Scattering in Random Media. New York: IEEE Press, 1997.
[25] S. Bloom, E. Korevaar, J. Schuster, and H. Willebrand, "Understanding the performance of free-space optics," Journal of Optical Networking, vol. 2, no. 6, pp. 178–200, 2003.
[26] H. Kaushal, V. K. Jain, and S. Kar, Free Space Optical Communication. New Delhi: Springer, 2017.
[27] made by ai agent from giminai and deep seek.

chapter 3 References

[1] S. Hitam, S. N. Suhaimi, A. S. M. Noor, S. B. A. Anas, and R. K. Z. Sahbudin, "Performance analysison 16-channels wavelength division multiplexing in free space optical transmission under tropical regions environment," J. Computer Sci., vol. 8, no. 1, pp. 145–148, 2012.1

[2] K. Arivazhagi and T. K. Shanthi, "An effective 8 × 7.5 Gbps WDM free space optical communication system," Int. J. Eng. Res. Technol. (IJERT), vol. 6, no. 8, pp. 1–5, 2018.

[3] E. E. Elsayed, "Design and analysis of a 1.28 Tbps DWDM free space optical link under atmospheric turbulence," J. Opt. Commun., 2021, doi:10.1515/joc-2021-0037.

[4] E. Ciaramella , "1.28 Tb/s (32×40 Gb/s) WDM transmission system for free-space optical communications," IEEE J. Sel. Areas Commun., vol. 27, no. 9, pp. 1639–1645, 2009.

[5] H. Song, D. Kim, and J. Lee, "4 × 10 Gb/s terrestrial FSO transmission over 1.2 km using an EDFA pre-amplifer and 100 GHz channel spacing," IEEE Photon. Technol. Lett., vol. 12, no. 6, pp. 690–692,2000.

[6] M. Y. Jeong , "8 × 10 Gb/s terrestrial FSO transmission over 3.4 km with an optical repeater," J. Opt.Soc. Korea, vol. 7, no. 2, pp. 89–94, 2003.

[7] H. Kaushal and G. Kaddoum, "Free space optical communication: Challenges and mitigation techniques," arXiv preprint arXiv:1506.04836, 2015.

[8] A. Prokes, "Atmospheric effects on the availability of free space optics systems," Opt. Eng., vol. 48,no. 6, p. 066001, 2009.

[9] V. W. S. Chan, "Free-space optical communications," J. Lightw. Technol., vol. 24, no. 12, pp. 4750–4762, 2006.

[10] U. A. Wakata, A. M. Haruna, S. A. Goni, and H. I. Usman, "Effects of atmospheric conditions on the quality of free space optical communication link in Nigeria," ARCN Int. J. Sustain. Dev., vol. 13, no. 1, pp. 47–54, 2020.

[11] A. Deyranlou and A. Maleki Javan, "Case study of a coherent FSO system with adaptive modulation for Isfahan climate," J. Opt. Commun., 2025, doi:10.1515/joc-2024-0037.

[12] M. A. A. Ali, "Performance analysis of terrestrial WDM-FSO under various weather conditions,"Wireless Sens. Netw., vol. 8, no. 4, pp. 33–44, 2016.

[13] F. Rashidi, J. He, and L. Chen, "Performance investigation of FSO-OFDM communication systems under heavy rain," in Proc. IEEE Int. Symp. Circuits Syst. (ISCAS), 2016, pp. 1234–1237.

[14] F. T. Mahmood, A. H. Ali, and A. H. A. Haeder, “Weather’s effect on the free space optics communication system,” Indonesian J. Electr. Eng. Comput. Sci., vol. 31, no. 1, pp. 222–228, 2023.
[15] I. I. Kim, R. Stieger, J. A. Koontz, C. Moursund, M. Barclay, and P. Adhikari , “Wireless optical transmission of fast ethernet, FDDI, ATM and ESCON protocol data using the TerraLink laser communication system,” Opt. Eng., vol. 37, no. 12, pp. 3143–3155, 1998.
[16] A. M. Abd El-Naser , “The effects of bad weather on the transmission of free space optical signals,”Int. J. Comput. Sci. Mob. Comput., 2012.